

Electronic Supplementary Information

Rhenium tricarbonyl complexes of AIE active tetraarylethylene ligands: tuning luminescence properties and HSA-specific binding

Moustafa T. Gabr and F. Christopher Pigge

Department of Chemistry, University of Iowa, Iowa City, Iowa 52242, United States

chris-pigge@uiowa.edu

Contents

UV-vis absorption spectrum of 2	S3
UV-vis absorption spectrum of 3	S3
UV-vis absorption spectrum of 4	S4
UV-vis absorption spectrum of 5	S4
UV-vis absorption spectrum of 6	S5
UV-vis absorption spectrum of 7	S5
UV-vis absorption spectrum of 8	S6
UV-vis absorption spectrum of 9	S6
UV-vis absorption spectrum of 10	S7
UV-vis absorption spectrum of 11	S7
UV-vis absorption spectrum of 12	S8
UV-vis absorption spectrum of 13	S8
UV-vis absorption spectrum of 14	S9
UV-vis absorption spectrum of 15	S9
UV-vis absorption spectrum of 16	S10
AIE profile of 2 in CH ₃ CN/H ₂ O mixtures	S10
AIE profile of 3 in CH ₃ CN/H ₂ O mixtures	S11
AIE profile of 4 in CH ₃ CN/H ₂ O mixtures	S11
AIE profile of 5 in CH ₃ CN/H ₂ O mixtures	S12
Emission spectra of 6 in degassed and aerated MeCN	S12
Emission spectra of 7 in degassed and aerated MeCN	S13
Emission spectra of 8 in degassed and aerated MeCN	S13
Emission spectra of 9 in degassed and aerated MeCN	S14

Emission spectra of 10 in degassed and aerated MeCN	S14
AIE profile of 11 in CH ₃ CN/PBS mixtures	S15
AIE profile of 12 in CH ₃ CN/PBS mixtures	S15
ACQ profile of 13 in CH ₃ CN/PBS mixtures	S16
AIE profile of 14 in CH ₃ CN/PBS mixtures	S16
ACQ profile of 15 in CH ₃ CN/PBS mixtures	S17
Dynamic light scattering results of 16 in 9:1 PBS:MeCN	S17
UV-vis absorption spectrum of 16 in MeCN and 9:1 PBS:MeCN	S18
UV-vis absorption spectrum of 16 in 9:1 PBS:MeCN over 48 hr period	S18
UV-vis absorption spectrum of 16 in 9:1 PBS:MeCN at pH 7.4 and 12.0	S19
UV-vis absorption spectrum of 17	S19
Overlay of UV-vis spectra of 16 and 17	S20
Emission response of 5 in presence of HSA	S20
Emission response of 11 in presence of HSA	S21
Emission response of 12 in presence of HSA	S21
Emission response of 13 in presence of HSA	S22
Emission response of 14 in presence of HSA	S22
Emission response of 15 in presence of HSA	S23
Emission response of 16 in presence of different amino acids	S23
Saturation binding assay of 16 towards HSA	S24
Emission response of 16 -HSA in presence of SDS	S24
Photophysical properties of 6-16	S25
X-ray crystallographic data for 12	S26
References	S27
IR spectra of 7, 8, 9, 11 and 12	S28
NMR spectra for all new compounds	S33

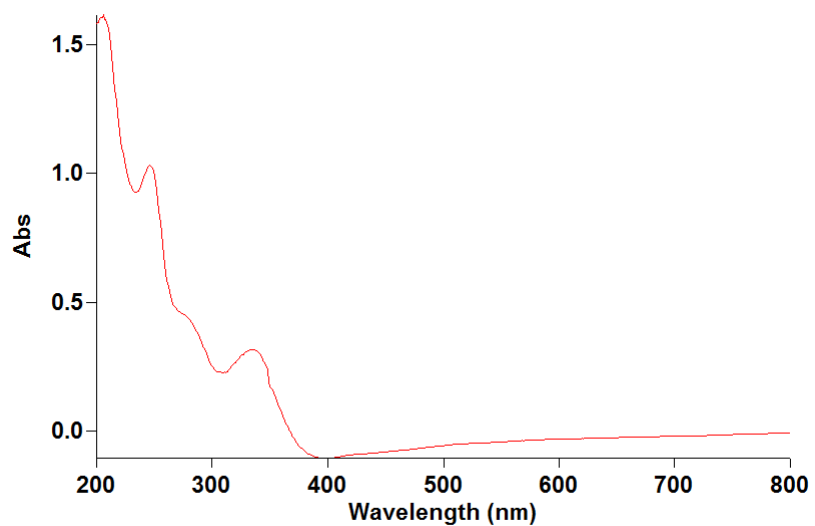


Figure S1. UV-vis absorption spectrum of **2** (CH_3CN , 25 μM).

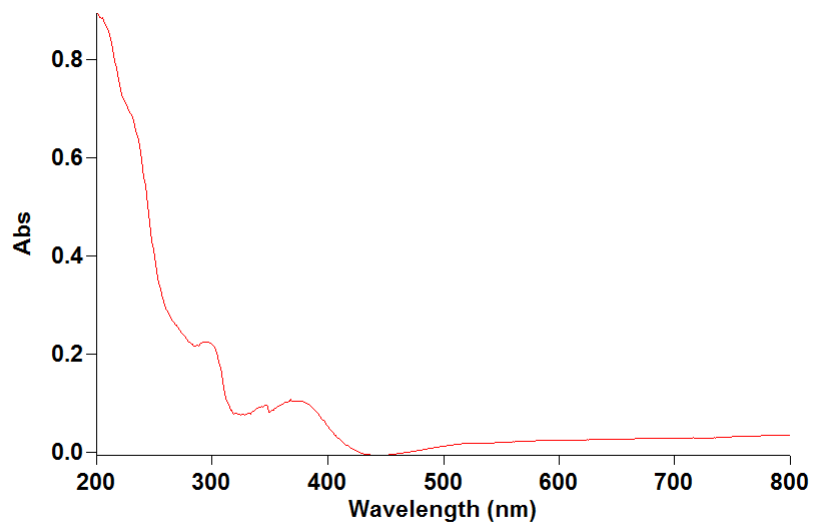


Figure S2. UV-vis absorption spectrum of **3** (CH_3CN , 12.5 μM).

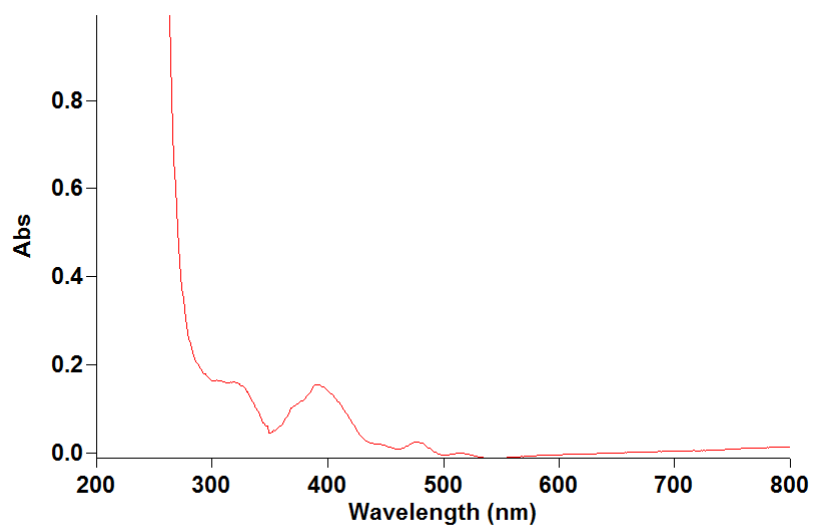


Figure S3. UV-vis absorption spectrum of **4** (CH_3CN , $12.5 \mu\text{M}$).

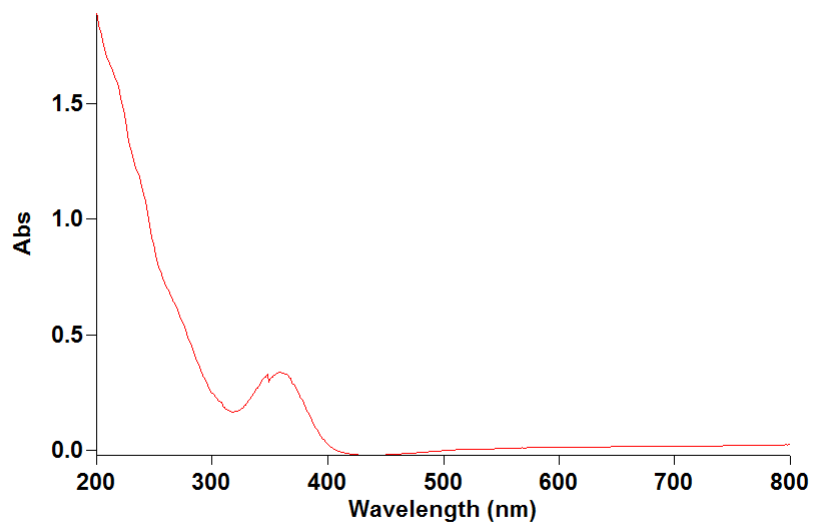


Figure S4. UV-vis absorption spectrum of **5** (CH_3CN , $25 \mu\text{M}$).

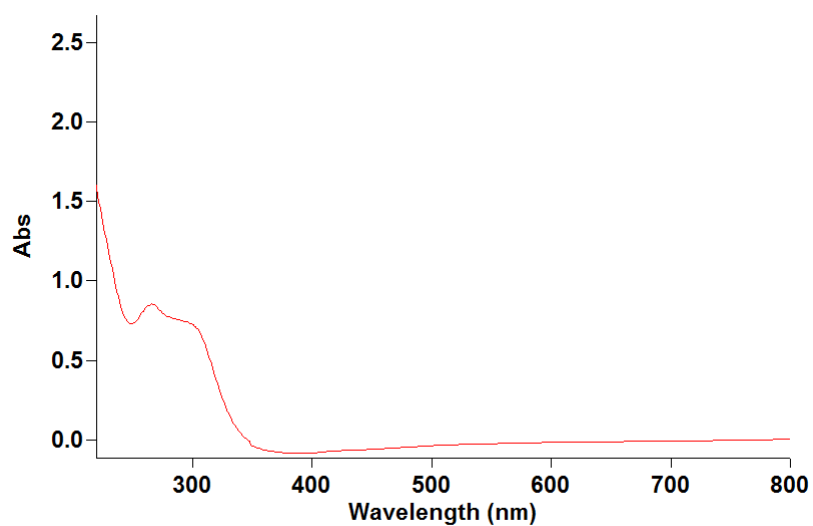


Figure S5. UV-vis absorption spectrum of **6** (CH_3CN , 50 μM).

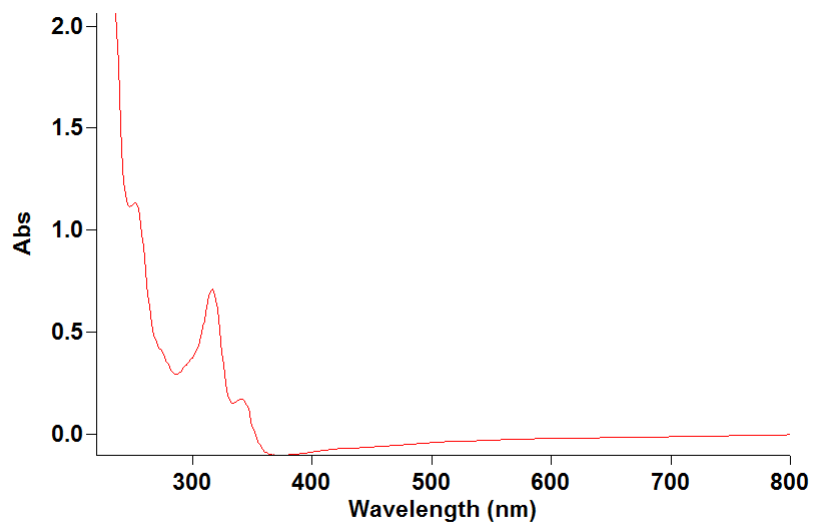


Figure S6. UV-vis absorption spectrum of **7** (CH_3CN , 25 μM).

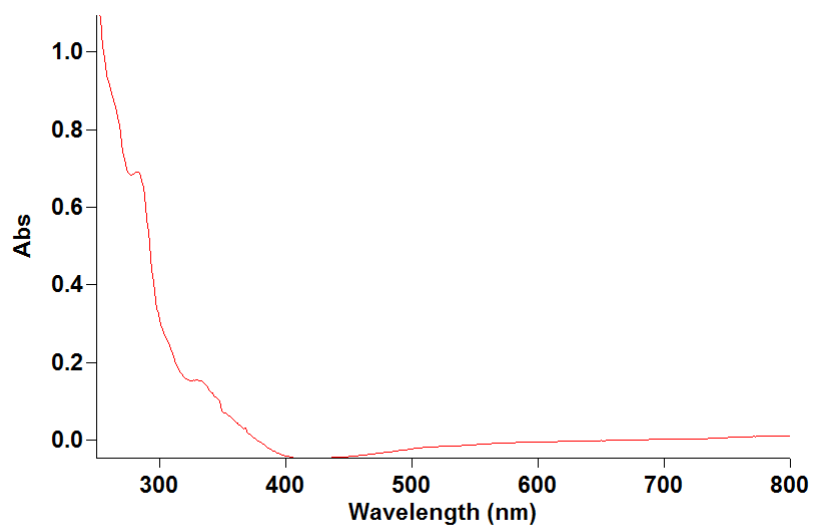


Figure S7. UV-vis absorption spectrum of **8** (CH_3CN , $12.5 \mu\text{M}$).

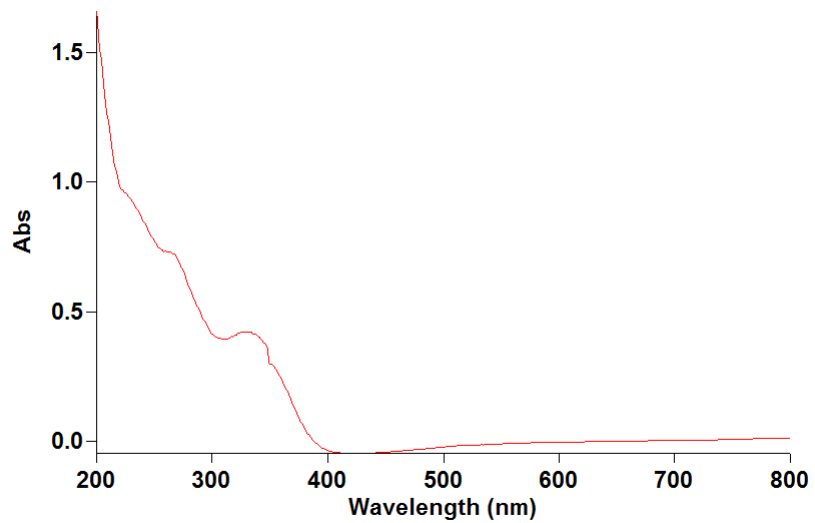


Figure S8. UV-vis absorption spectrum of **9** (CH_3CN , $25 \mu\text{M}$).

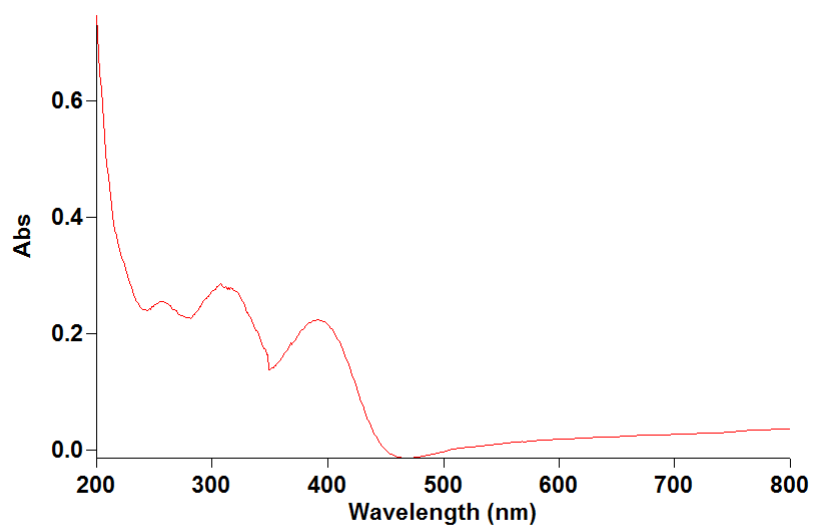


Figure S9. UV-vis absorption spectrum of **10** (CH_3CN , 12.5 μM).

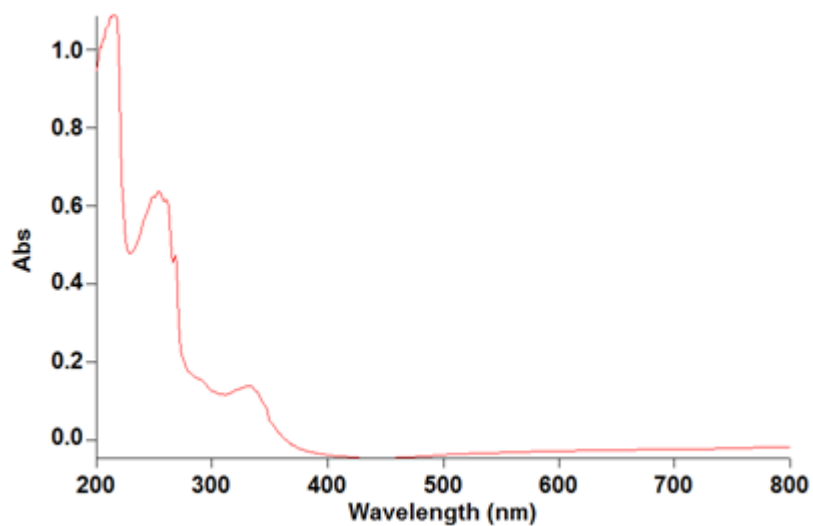


Figure S10. UV-vis absorption spectrum of **11** (CH_3CN , 12.5 μM).

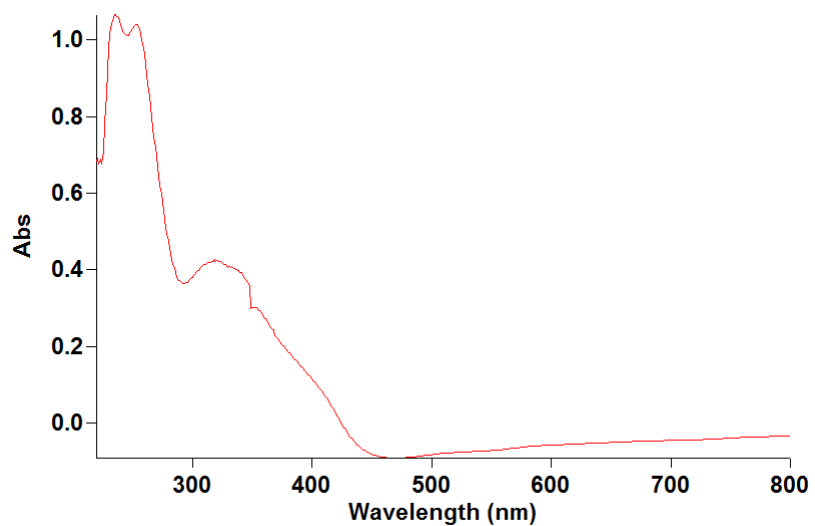


Figure S11. UV-vis absorption spectrum of **12** (CH_3CN , $12.5 \mu\text{M}$).

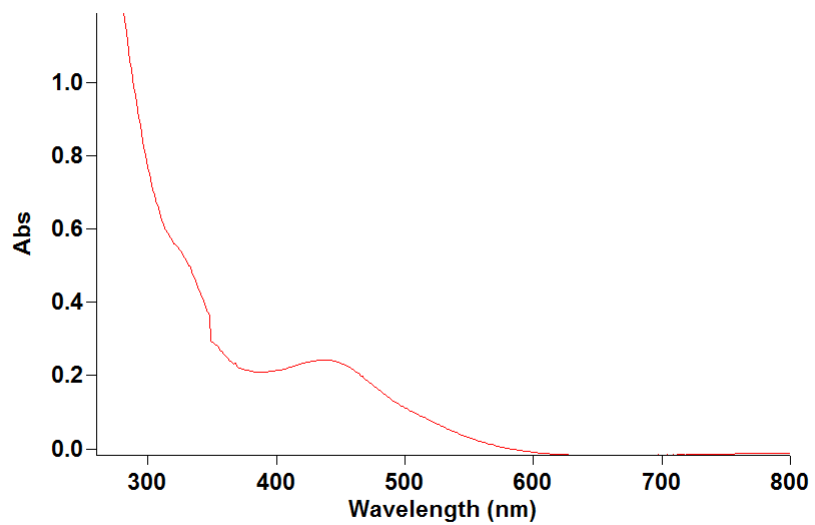


Figure S12. UV-vis absorption spectrum of **13** (CH_3CN , $12.5 \mu\text{M}$).

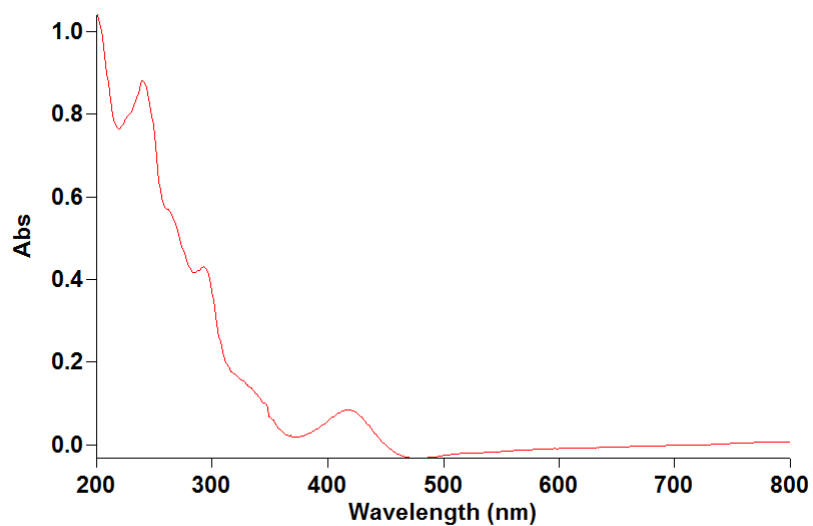


Figure S13. UV-vis absorption spectrum of **14** (CH_3CN , 12.5 μM).

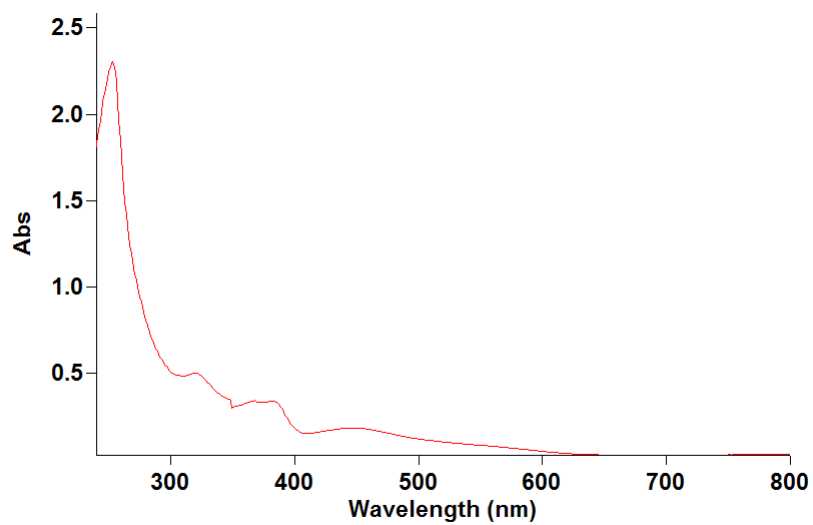


Figure S14. UV-vis absorption spectrum of **15** (CH_3CN , 12.5 μM).

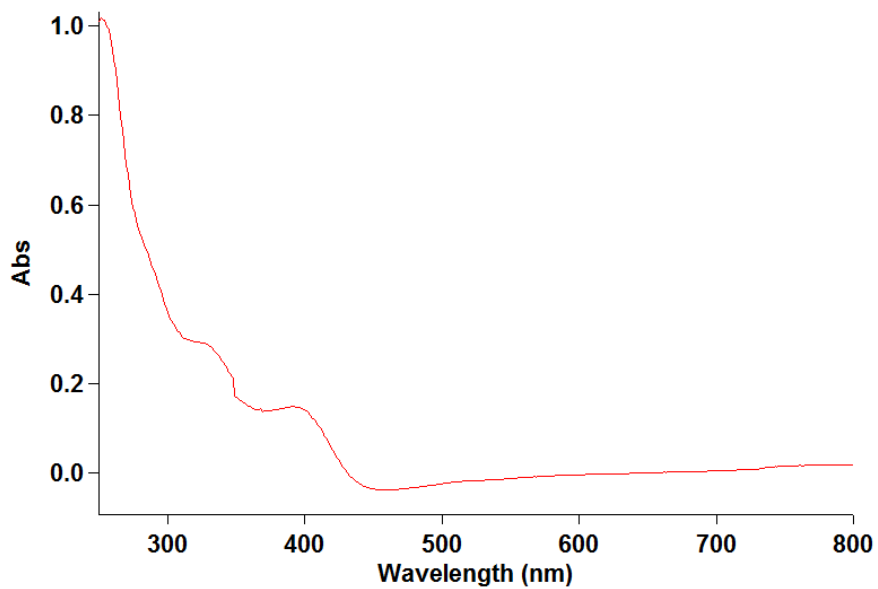


Figure S15. UV-vis absorption spectrum of **16** (CH_3CN , $12.5 \mu\text{M}$).

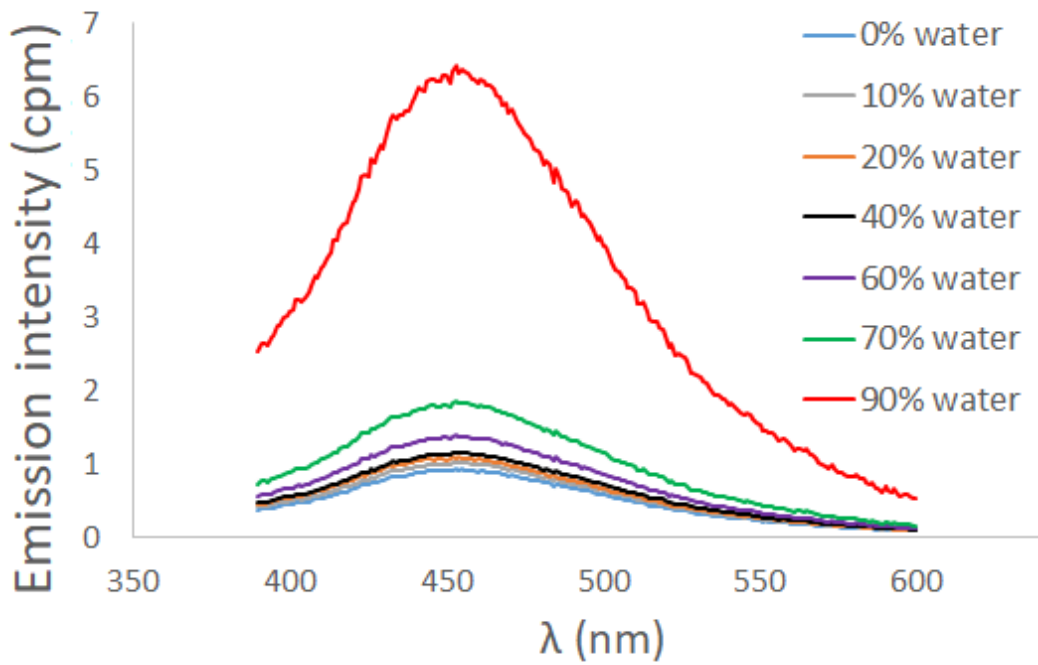


Figure S16. AIE profile of **2** in $\text{CH}_3\text{CN}/\text{H}_2\text{O}$ mixtures. $\lambda_{\text{ex}} = 318 \text{ nm}$, $[\mathbf{2}] = 10 \mu\text{M}$.

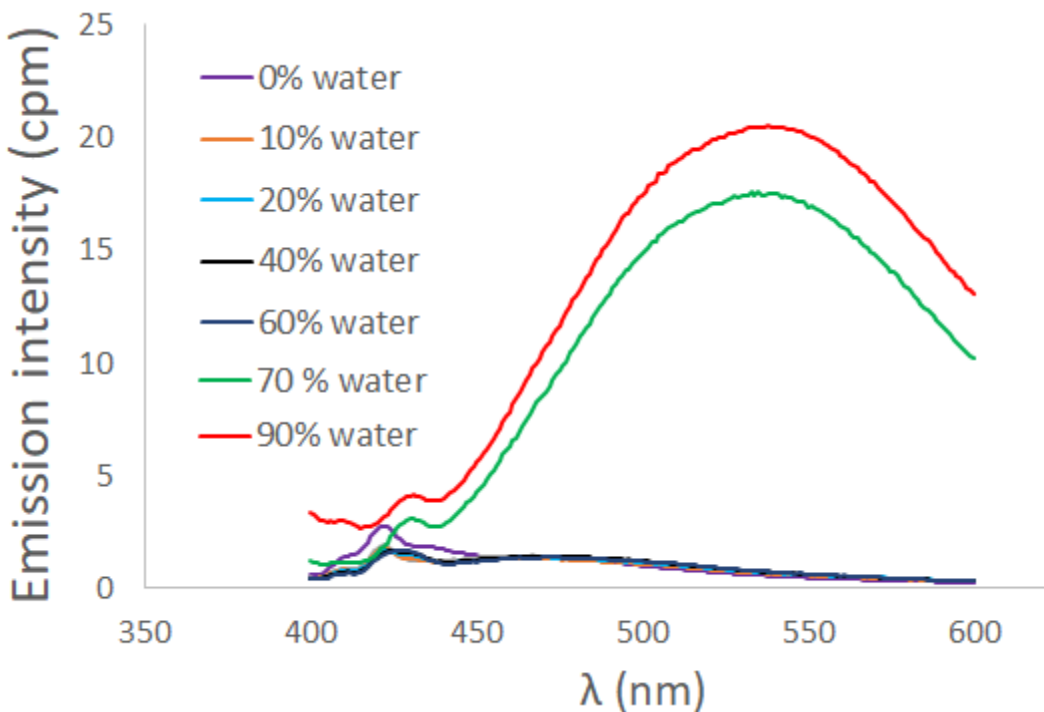


Figure S17. AIE profile of **3** in $\text{CH}_3\text{CN}/\text{H}_2\text{O}$ mixtures. $\lambda_{\text{ex}} = 367 \text{ nm}$, $[\mathbf{3}] = 10 \mu\text{M}$.

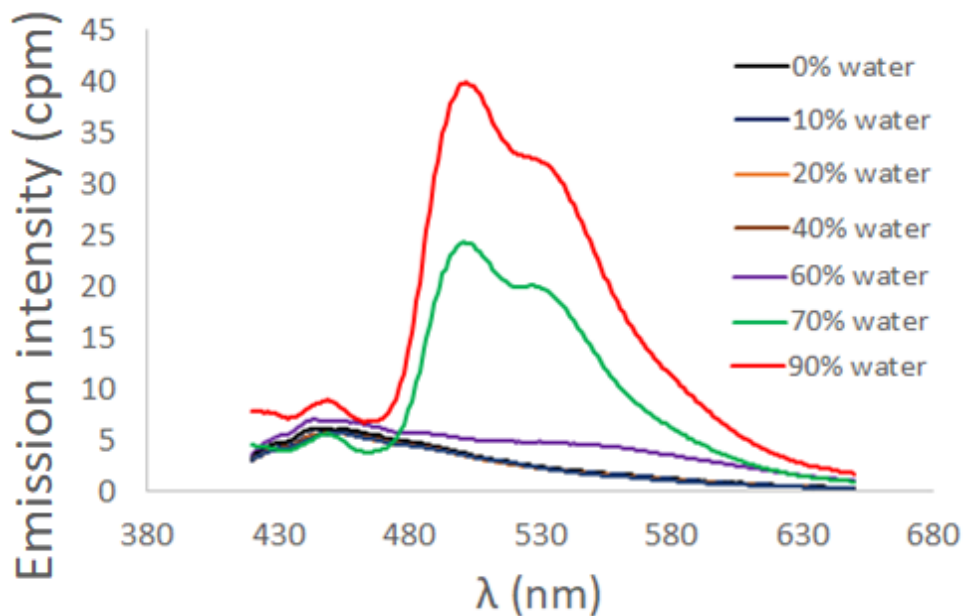


Figure S18. AIE profile of **4** in $\text{CH}_3\text{CN}/\text{H}_2\text{O}$ mixtures. $\lambda_{\text{ex}} = 393 \text{ nm}$, $[\mathbf{4}] = 10 \mu\text{M}$.

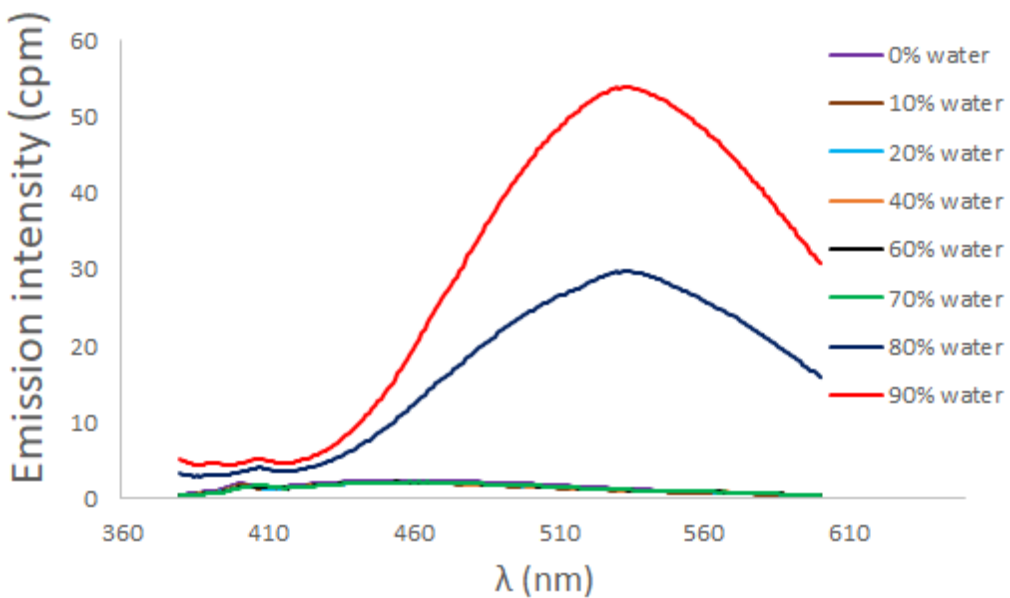


Figure S19. AIE profile of **5** in $\text{CH}_3\text{CN}/\text{H}_2\text{O}$ mixtures. $\lambda_{\text{ex}} = 354 \text{ nm}$, $[\mathbf{5}] = 10 \mu\text{M}$.

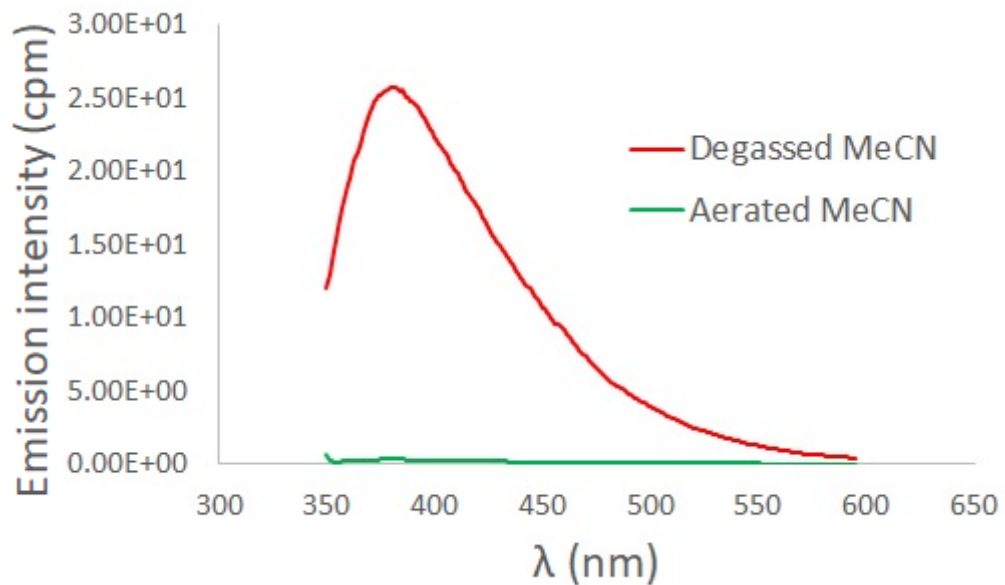


Figure S20. Emission spectra of **6** in degassed and aerated MeCN. $\lambda_{\text{ex}} = 326 \text{ nm}$, $[\mathbf{6}] = 10 \mu\text{M}$.

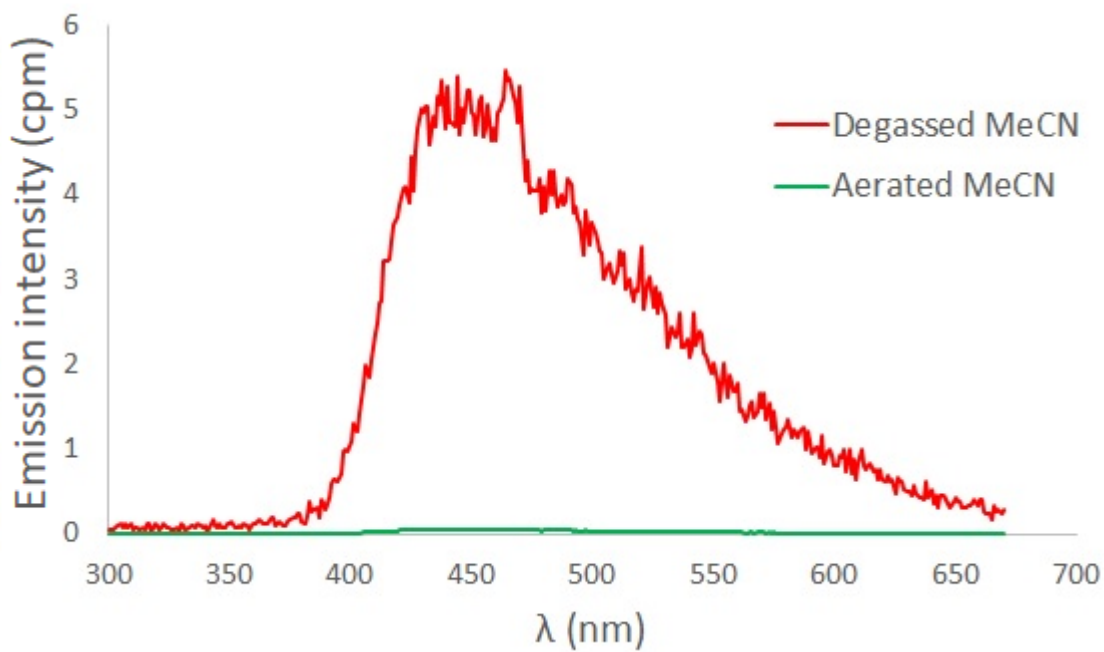


Figure S21. Emission spectra of **7** in degassed and aerated MeCN. $\lambda_{\text{ex}} = 340$ nm, $[7] = 10 \mu\text{M}$.

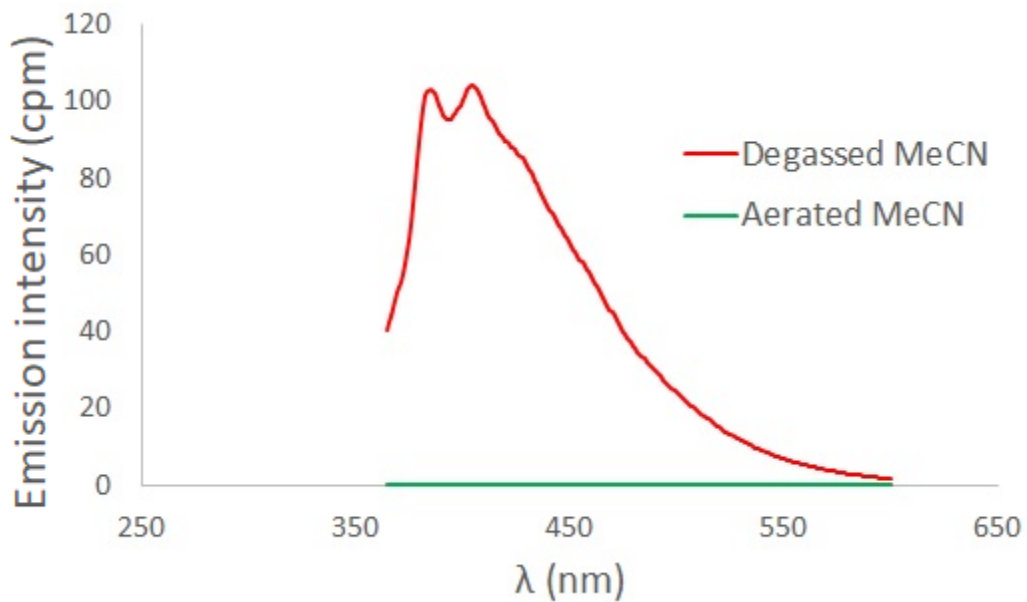


Figure S22. Emission spectra of **8** in degassed and aerated MeCN. $\lambda_{\text{ex}} = 337$ nm, $[8] = 10 \mu\text{M}$.

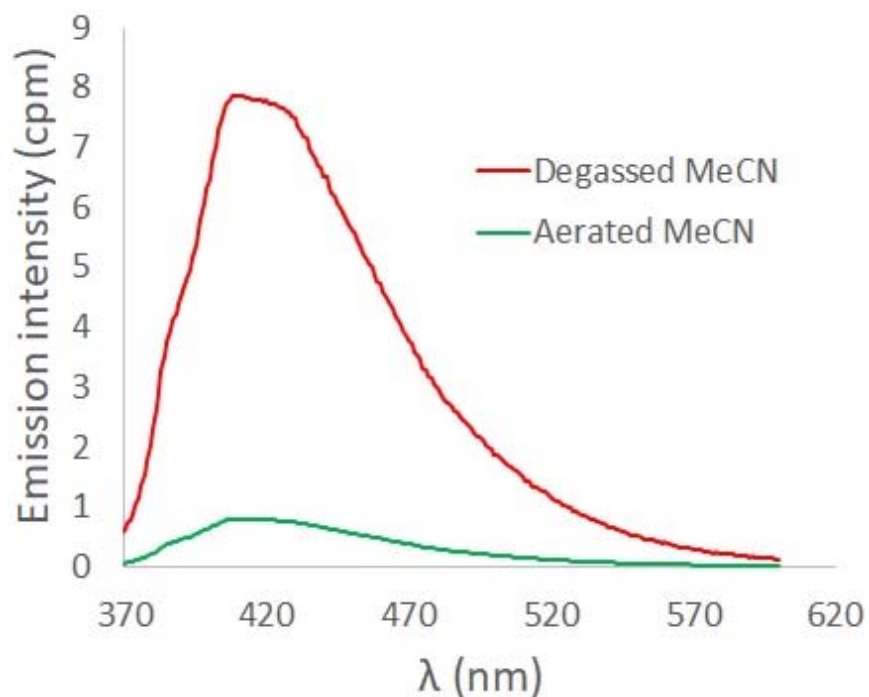


Figure S23. Emission spectra of **9** in degassed and aerated MeCN. $\lambda_{\text{ex}} = 341 \text{ nm}$, $[\mathbf{9}] = 10 \mu\text{M}$.

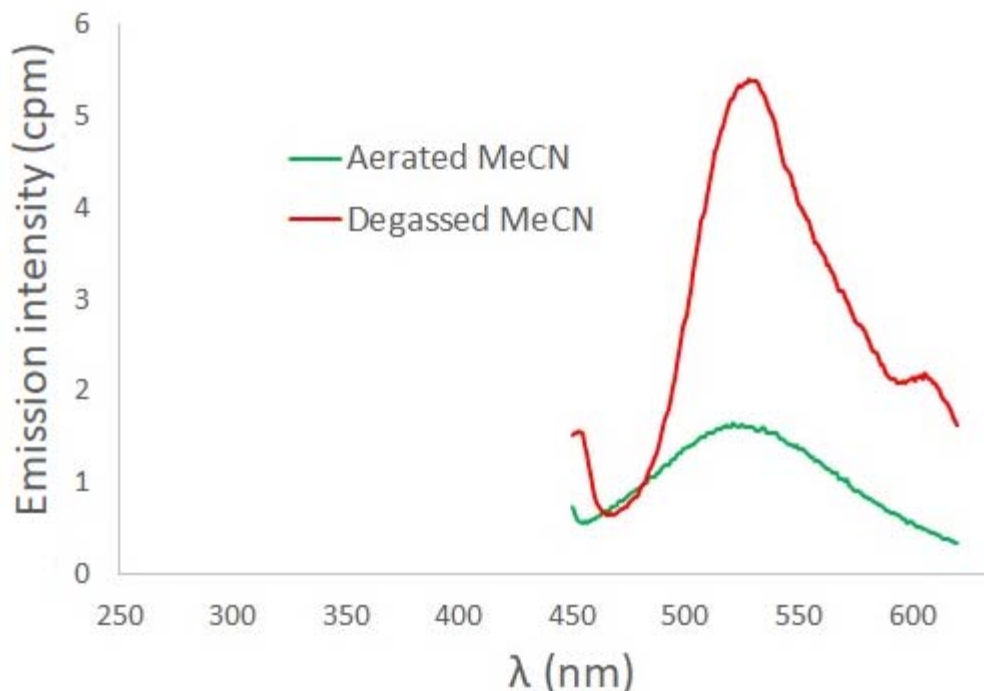


Figure S24. Emission spectra of **10** in degassed and aerated MeCN. $\lambda_{\text{ex}} = 394 \text{ nm}$, $[\mathbf{10}] = 10 \mu\text{M}$.

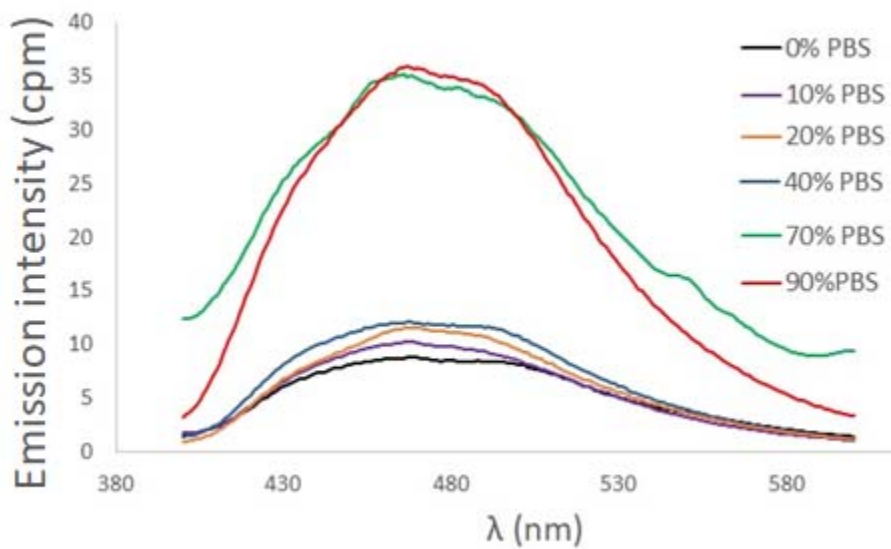


Figure S25. AIE profile of **11** in $\text{CH}_3\text{CN}/\text{PBS}$ ($\text{PH}=7.4$) mixtures. $\lambda_{\text{ex}} = 334 \text{ nm}$, $[\mathbf{11}] = 10 \mu\text{M}$

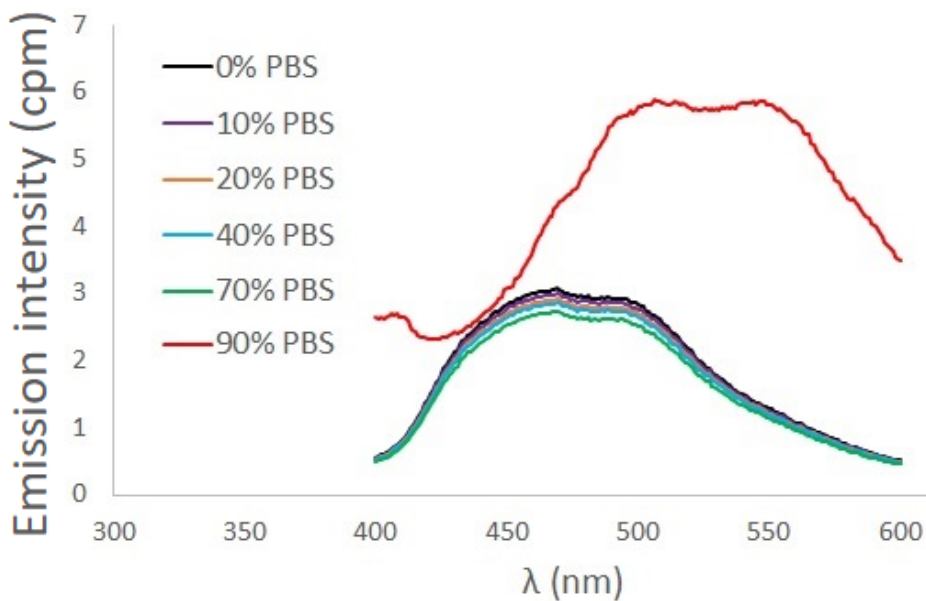


Figure S26. AIE profile of **12** in $\text{CH}_3\text{CN}/\text{PBS}$ ($\text{PH}=7.4$) mixtures. $\lambda_{\text{ex}} = 364 \text{ nm}$, $[\mathbf{12}] = 10 \mu\text{M}$.

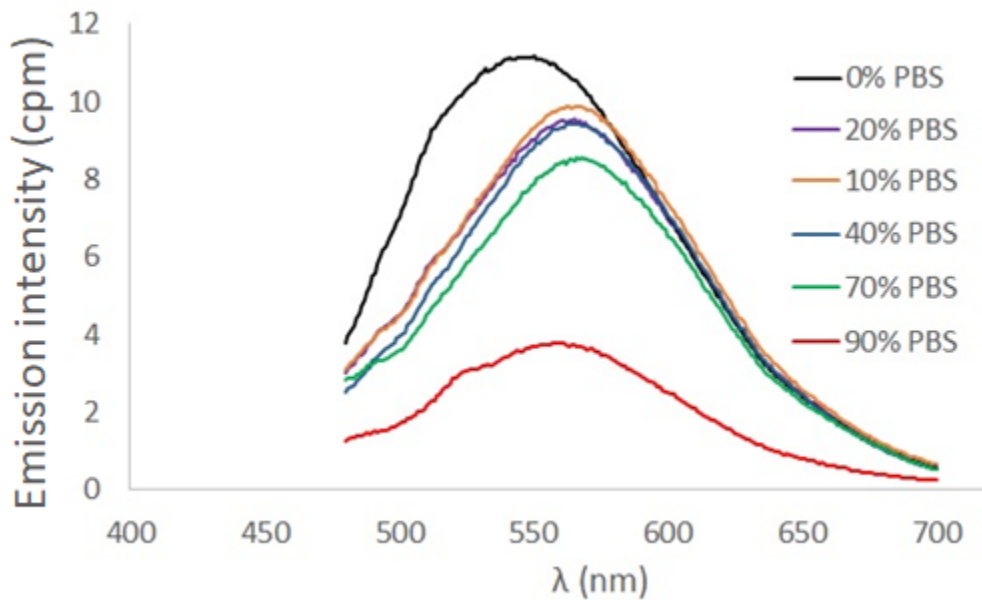


Figure S27. ACQ profile of **13** in $\text{CH}_3\text{CN}/\text{PBS}$ ($\text{PH}=7.4$) mixtures. $\lambda_{\text{ex}} = 447 \text{ nm}$, $[\mathbf{13}] = 10 \mu\text{M}$.

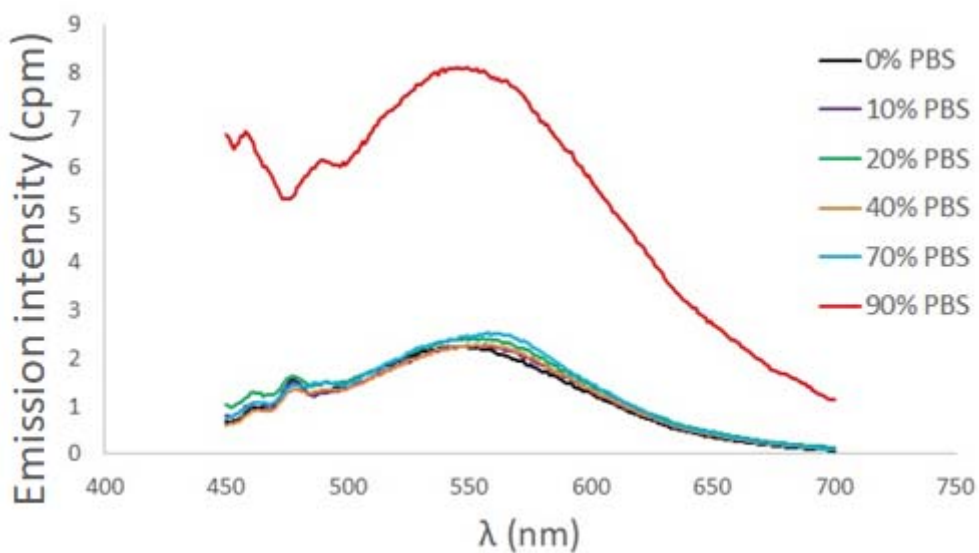


Figure S28. AIE profile of **14** in $\text{CH}_3\text{CN}/\text{PBS}$ mixtures ($\text{PH}=7.4$). $\lambda_{\text{ex}} = 419 \text{ nm}$, $[\mathbf{14}] = 10 \mu\text{M}$.

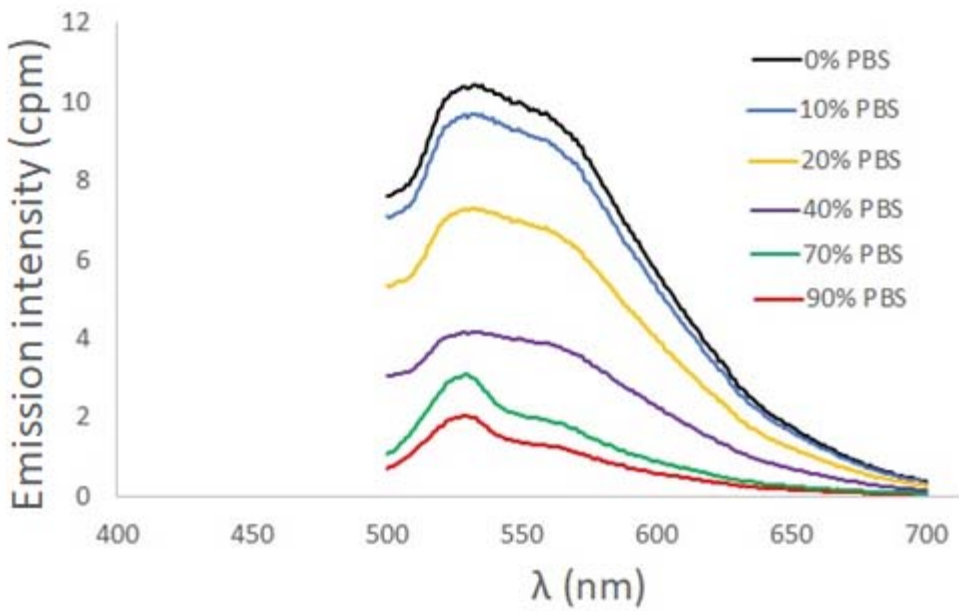


Figure S29. ACQ profile of **15** in $\text{CH}_3\text{CN}/\text{PBS}$ mixtures ($\text{pH} = 7.4$). $\lambda_{\text{ex}} = 450 \text{ nm}$, $[\mathbf{15}] = 10 \mu\text{M}$.

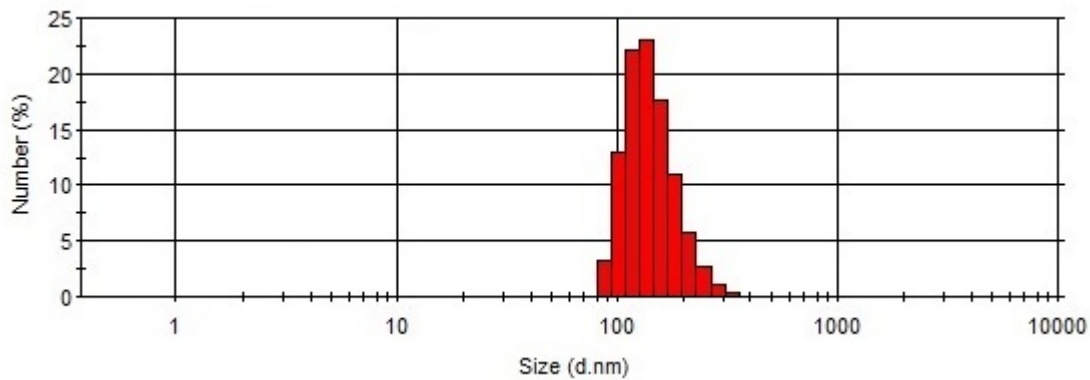


Figure S30. Dynamic light scattering results of **16** ($10 \mu\text{M}$) in 9:1 PBS:MeCN.

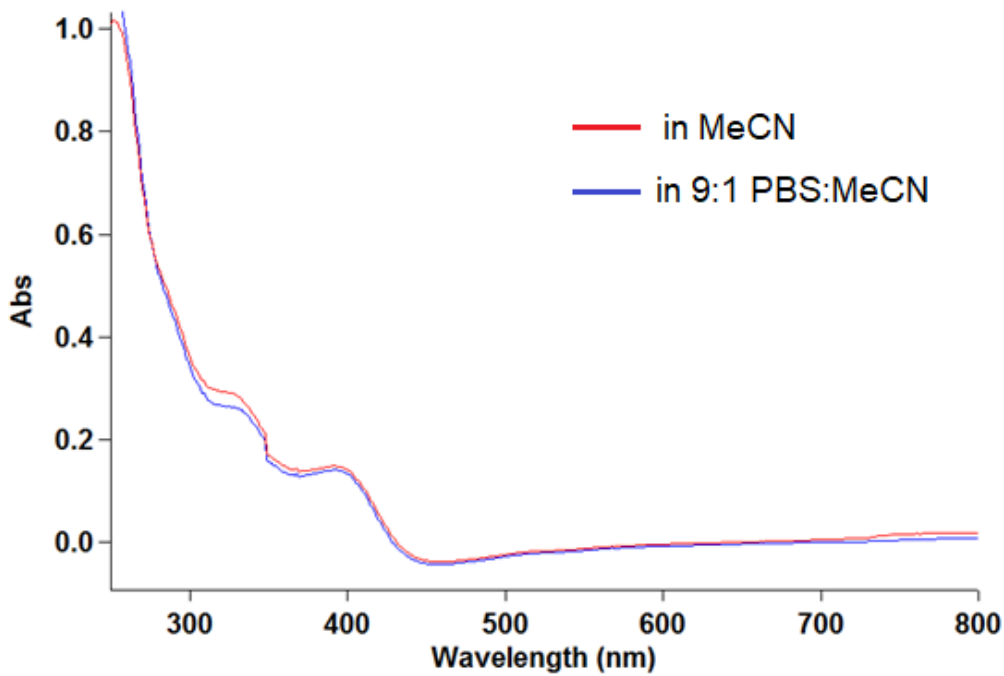


Figure S31. UV-vis absorption spectrum of **16** (12.5 μ M) in MeCN and 9:1 PBS:MeCN.

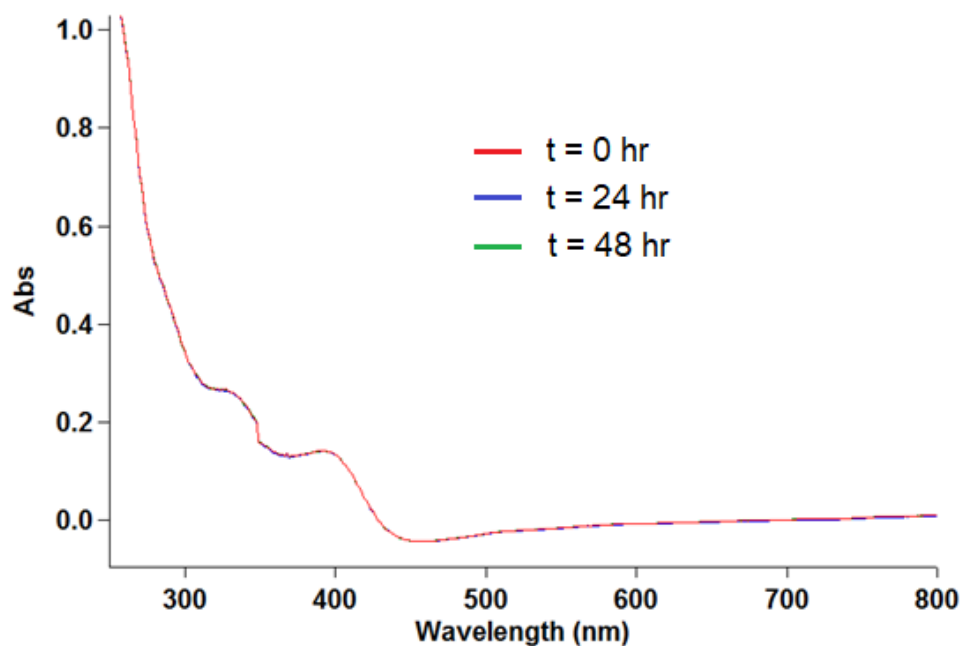


Figure S32. UV-vis absorption spectrum of **16** (12.5 μ M, 9:1 PBS:MeCN) over 48 hr period.

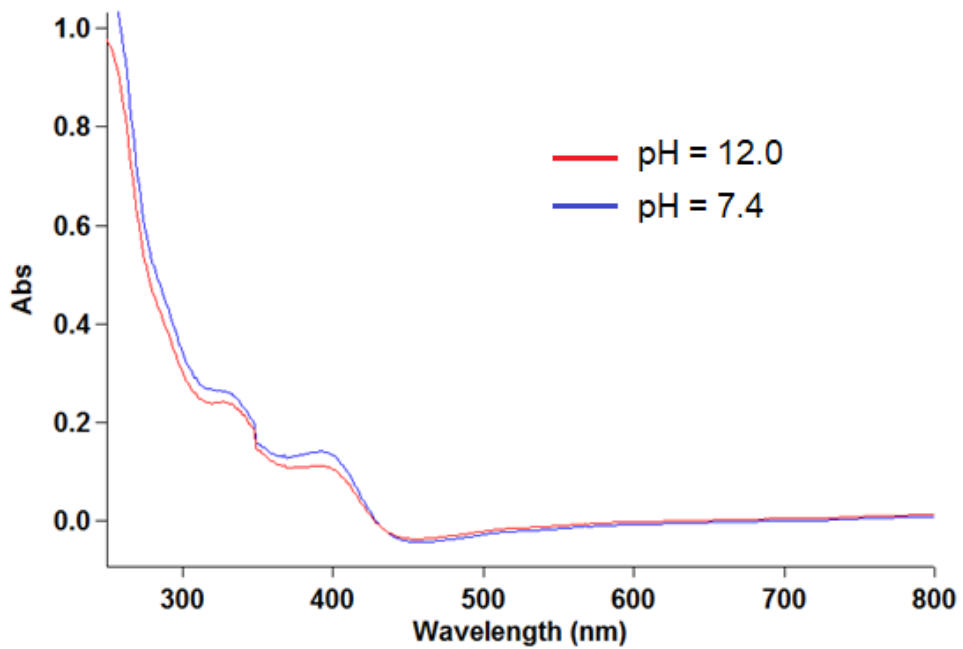


Figure S33. UV-vis absorption spectrum of **16** (12.5 μ M, 9:1 PBS:MeCN) at pH = 7.4 and 12.0.

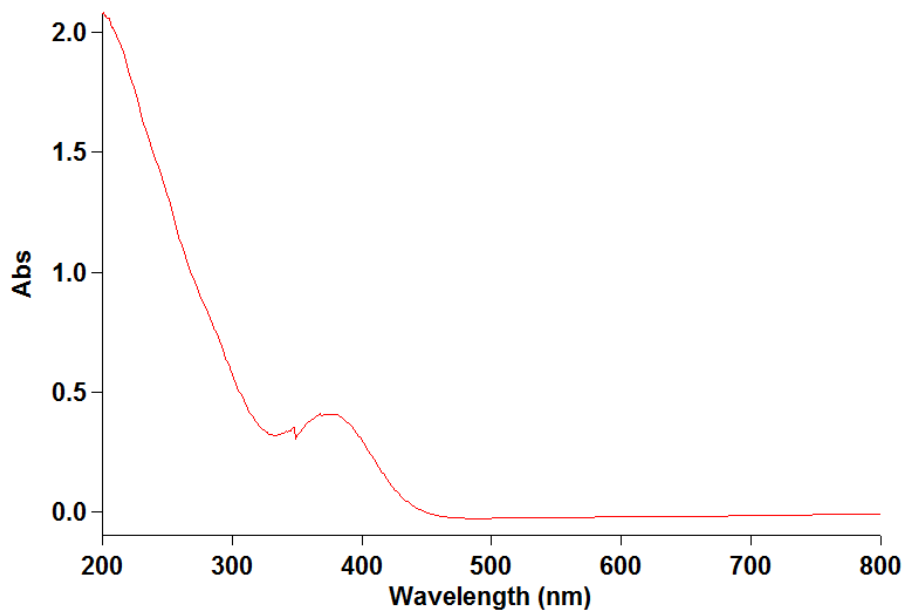


Figure S34. UV-vis absorption spectrum of **17** (MeCN, 25 μ M).

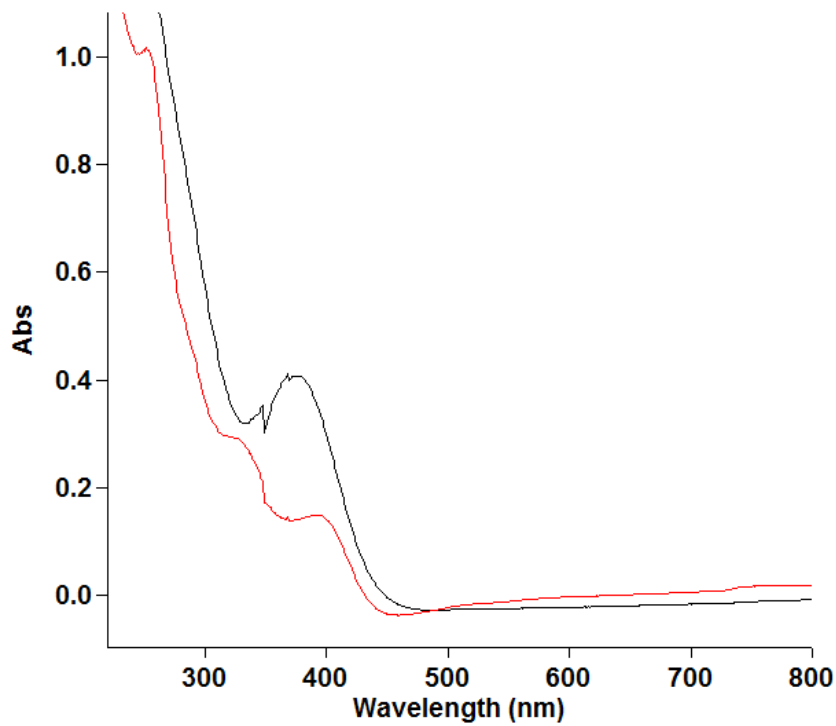


Figure S35. Overlay of UV-vis absorption spectra of **16** (MeCN, 12.5 μM) in red and **17** (MeCN, 25 μM) in black.

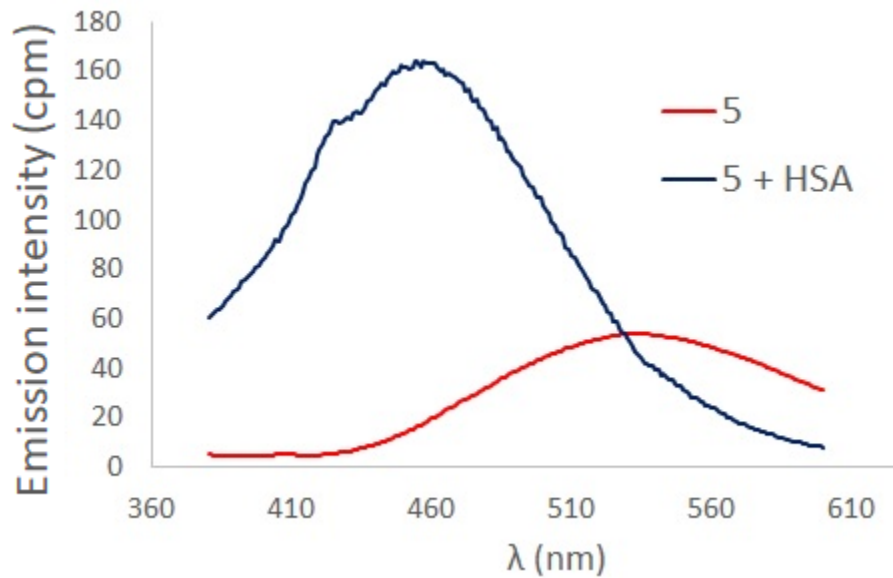


Figure S36. Emission response of **5** in presence and absence of 20 μM HSA in 9:1 PBS:MeCN (PH= 7.4). $\lambda_{\text{ex}} = 354$ nm, $[5] = 10$ μM .

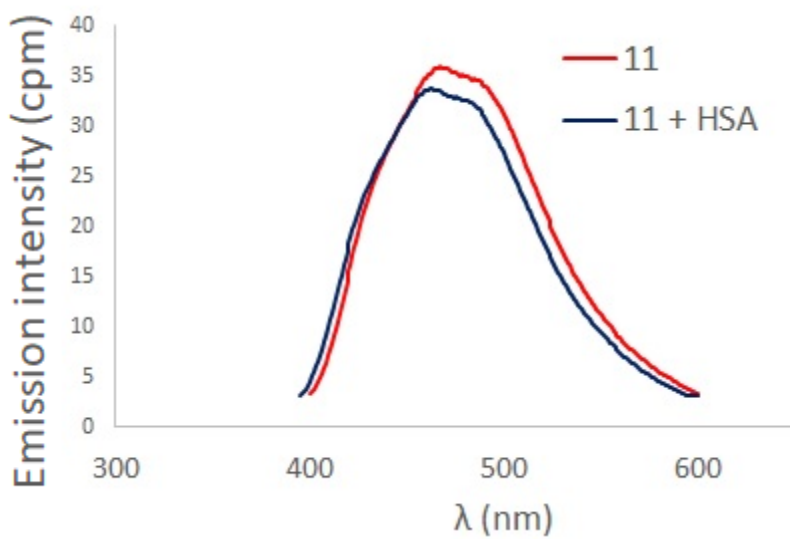


Figure S37. Emission response of **11** in presence and absence of 20 μM HSA in 9:1 PBS:MeCN (PH=7.4). $\lambda_{\text{ex}} = 334 \text{ nm}$, $[\mathbf{11}] = 10 \mu\text{M}$.

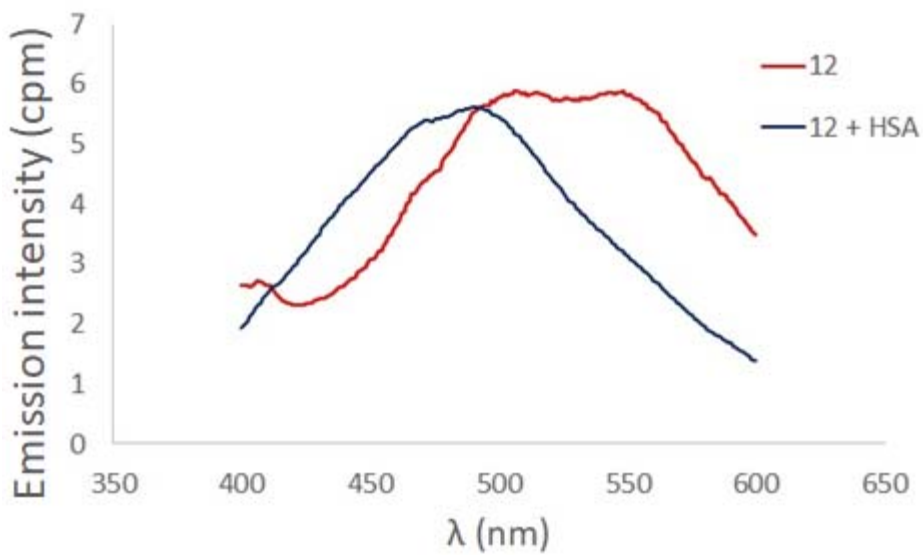


Figure S38. Emission response of **12** in presence and absence of 20 μM HSA in 9:1 PBS:MeCN (PH=7.4). $\lambda_{\text{ex}} = 364 \text{ nm}$, $[\mathbf{12}] = 10 \mu\text{M}$.

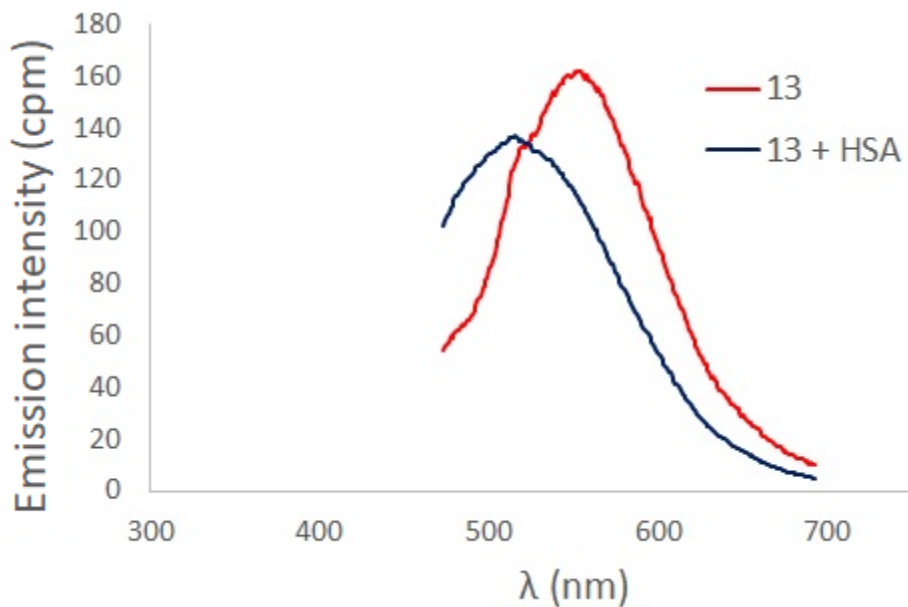


Figure S39. Emission response of **13** in presence and absence of 20 μM HSA in 9:1 PBS:MeCN (PH=7.4). $\lambda_{\text{ex}} = 447 \text{ nm}$, $[\mathbf{13}] = 10 \mu\text{M}$.

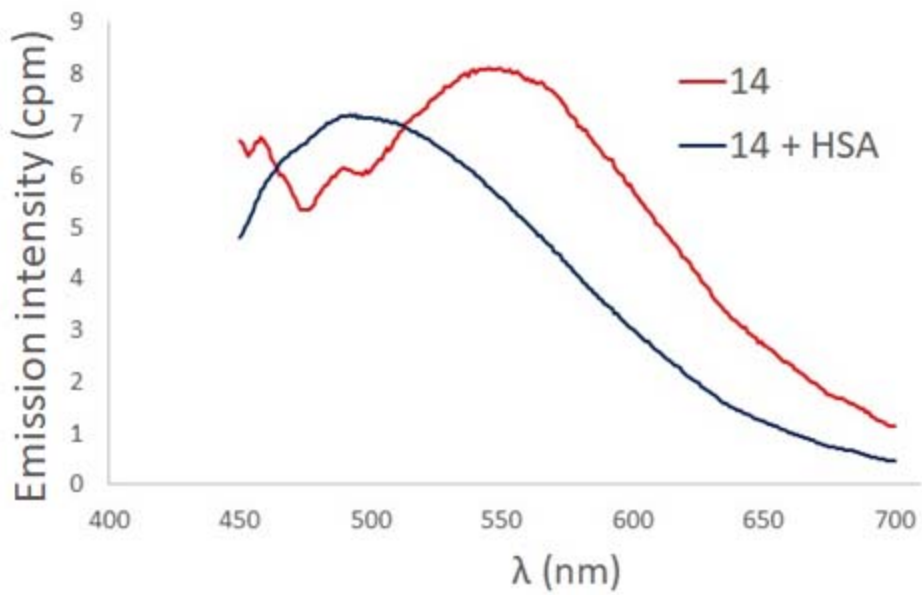


Figure S40. Emission response of **14** in presence and absence of 20 μM HSA in 9:1 PBS:MeCN (PH=7.4). $\lambda_{\text{ex}} = 419 \text{ nm}$, $[\mathbf{14}] = 10 \mu\text{M}$.

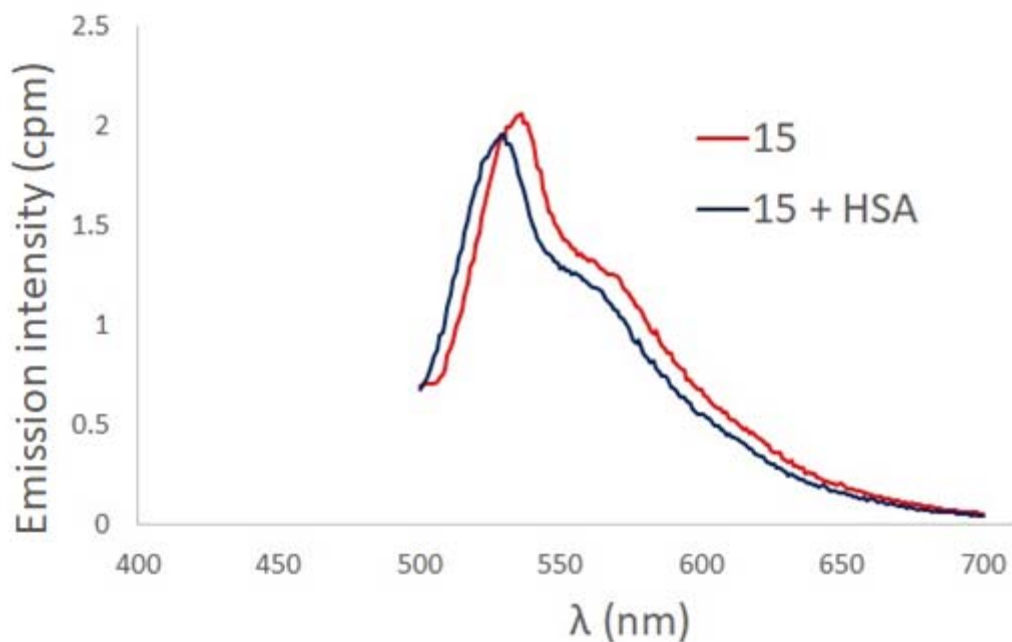


Figure S41. Emission response of **15** in presence and absence of 20 μM HSA in 9:1 PBS:MeCN (PH=7.4). $\lambda_{\text{ex}} = 450 \text{ nm}$, $[\mathbf{15}] = 10 \mu\text{M}$.

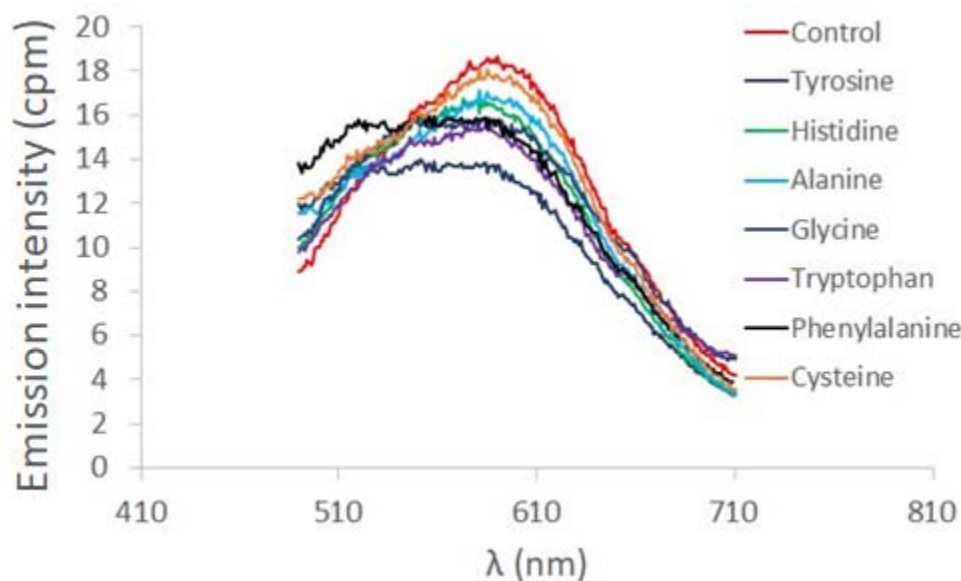


Figure S42. Emission response of **16** in presence and absence of different amino acids in 9:1 PBS:MeCN (PH=7.4). $\lambda_{\text{ex}} = 396 \text{ nm}$, $[\mathbf{16}] = 10 \mu\text{M}$.

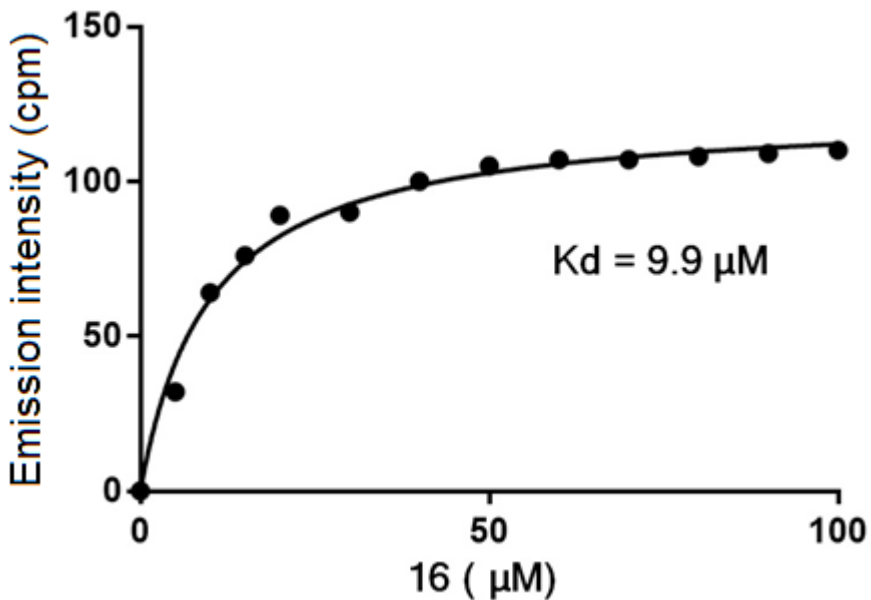


Figure S43. Saturation binding assay generated by GraphPad Prism using various concentrations of **16** (0-100 μM) towards HSA (20 μM).

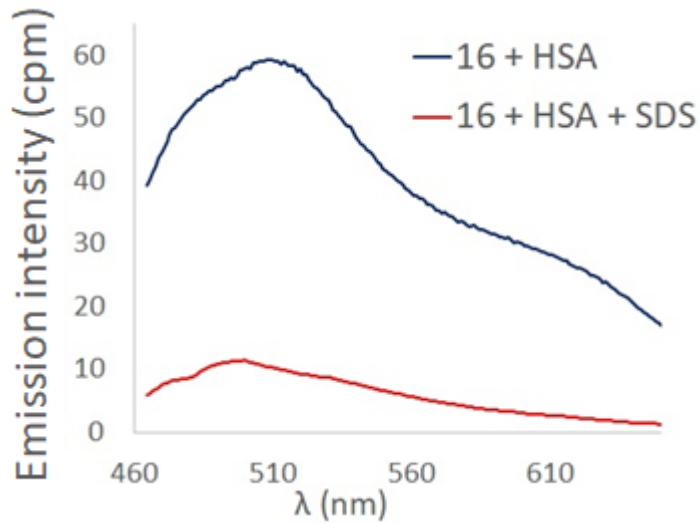


Figure S44. Emission response of **16**.HSA complex in presence and absence of SDS (20 μM) in 9:1 PBS:MeCN (PH= 7.4). $\lambda_{\text{ex}} = 396$ nm, $[\mathbf{16}] = 10 \mu\text{M}$, $[\text{HSA}] = 20 \mu\text{M}$.

Table S1. Photophysical properties of **6-16**.

<i>Compound No.</i>	λ_{ex} in MeCN (nm)	λ_{em} in MeCN (nm)	λ_{em} in MeCN: PBS (1:9) (nm)	Stokes shift (MeCN)	Φ (%) in aerated MeCN ^a	Φ (%) in degassed MeCN ^a	Φ (%) in MeCN: PBS (1:9) ^a
6	326	385	nd ^b	59	nd	3.2	nd
7	340	444	nd	104	nd	2.1	nd
8	337	410	nd	73	nd	3.7	nd
9	341	420	423	79	0.7	4.1	1.1
10	394	526	529	132	1.4	6.3	1.4
11	334	474	476	140	3.1	8.1	11.5
12	364	469	518	105	5.1	9.4	10.1
13	447	547	563	100	6.2	12.1	1.6
14	419	543	549	124	6.8	17.4	19.8
15	450	527	521	77	8.4	14.5	1.4
16	396	505	595	109	3.8	10.3	10.7

^a Quantum yields calculated using tris(2,2'-bipyridyl)ruthenium(II) chloride in aerated water ($\Phi = 2.8\%$)¹ as a reference.

^bnd: not determined.

Table 2. Crystallographic data for **12**.

Formula	C ₃₁ H ₁₈ CIN ₂ O ₃ ReS ₂ ,C ₇ H ₈
FW	844.38
Crystal System	Triclinic
Space group	P -1
a/Å	8.7755(9)
b/Å	13.4717(14)
c/Å	15.1412(15)
α/°	78.884(5)
β/°	77.789(5)
γ/°	72.824(5)
V/Å ³	1655.11(16)
Z	2
D _{calc}	1.694
μ (mm ⁻¹)	3.919
T/K	190.15
No. of reflections	30896
No. of unique reflections	9988
No. of reflections with I > 2σ(I)	7097
R ₁ [I > 2σ(I)]	0.0185
wR ₂	0.0408
CCDC No.	1571905

This complex crystallized with a full molecule in the asymmetric unit along with one full disordered toluene solvate molecule. One thiophene ring is disordered by a two-fold rotation about the C5-C11 bond. The C5-C11 and C5-C11' bonds were restrained to be the same. The anisotropic displacement parameters (adp's) of the disordered pair were restrained by the rigid bond and similarity restraints. The toluene molecule was disordered over an inversion center with two positions that are coplanar and in a 180° angle relative to each other. Toluene solvate was refined by using geometry restraints with two positions for each atom.

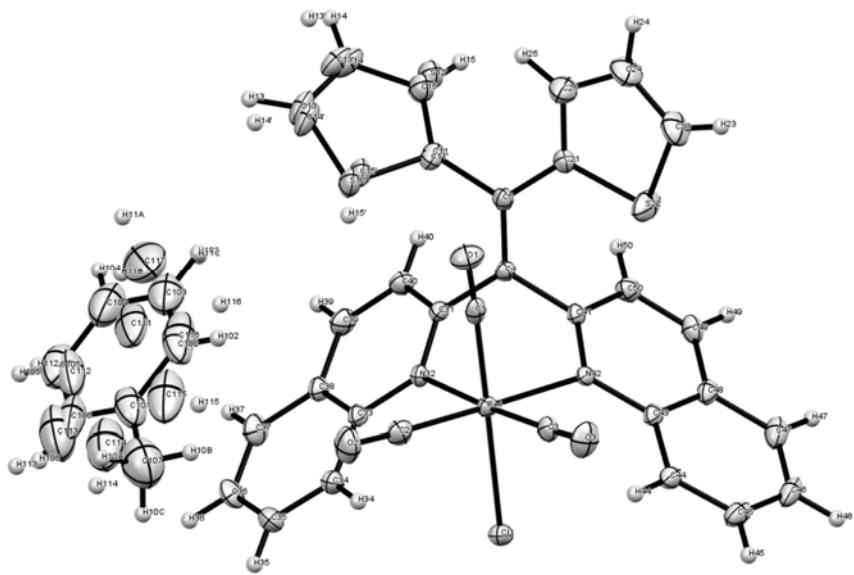
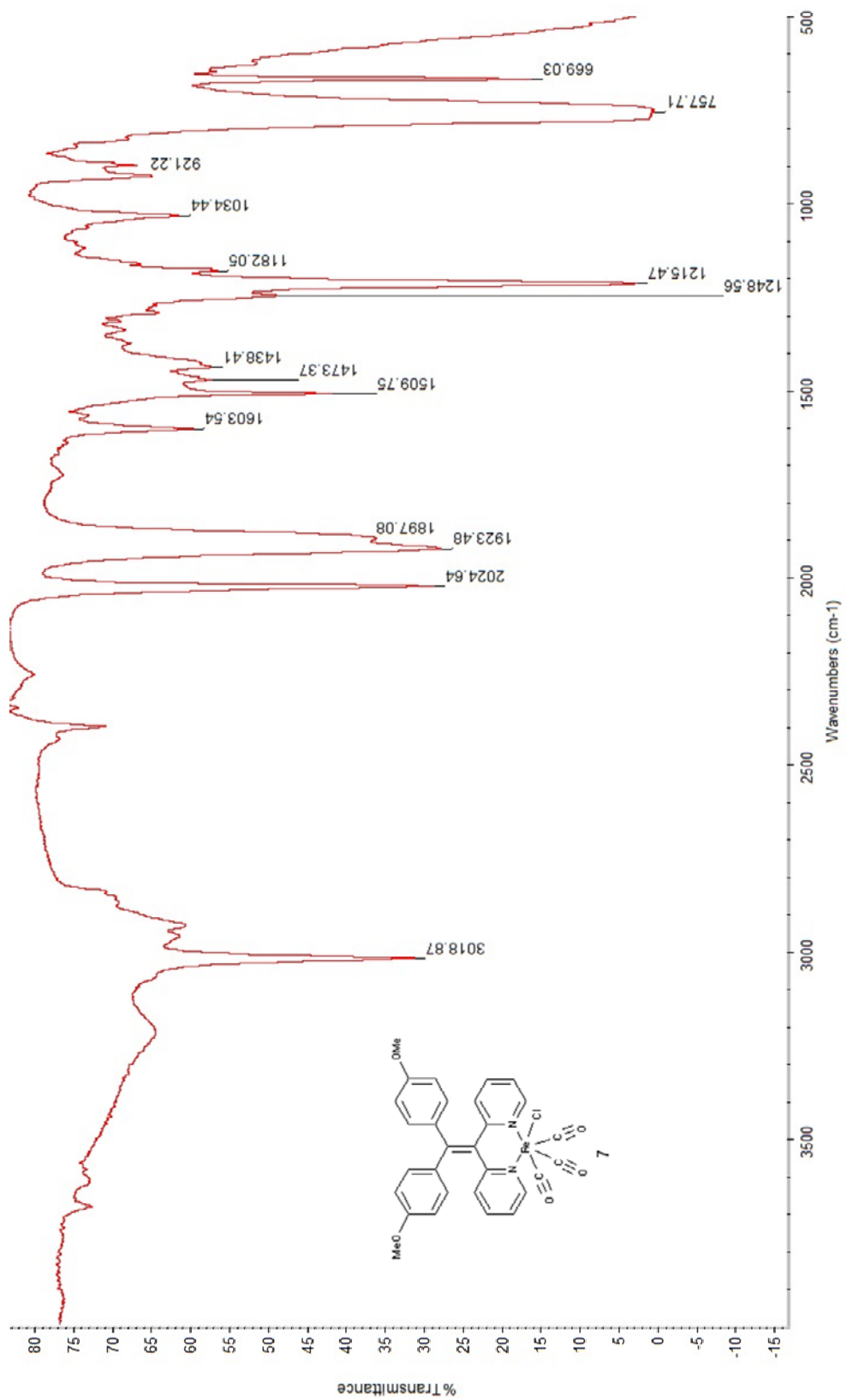
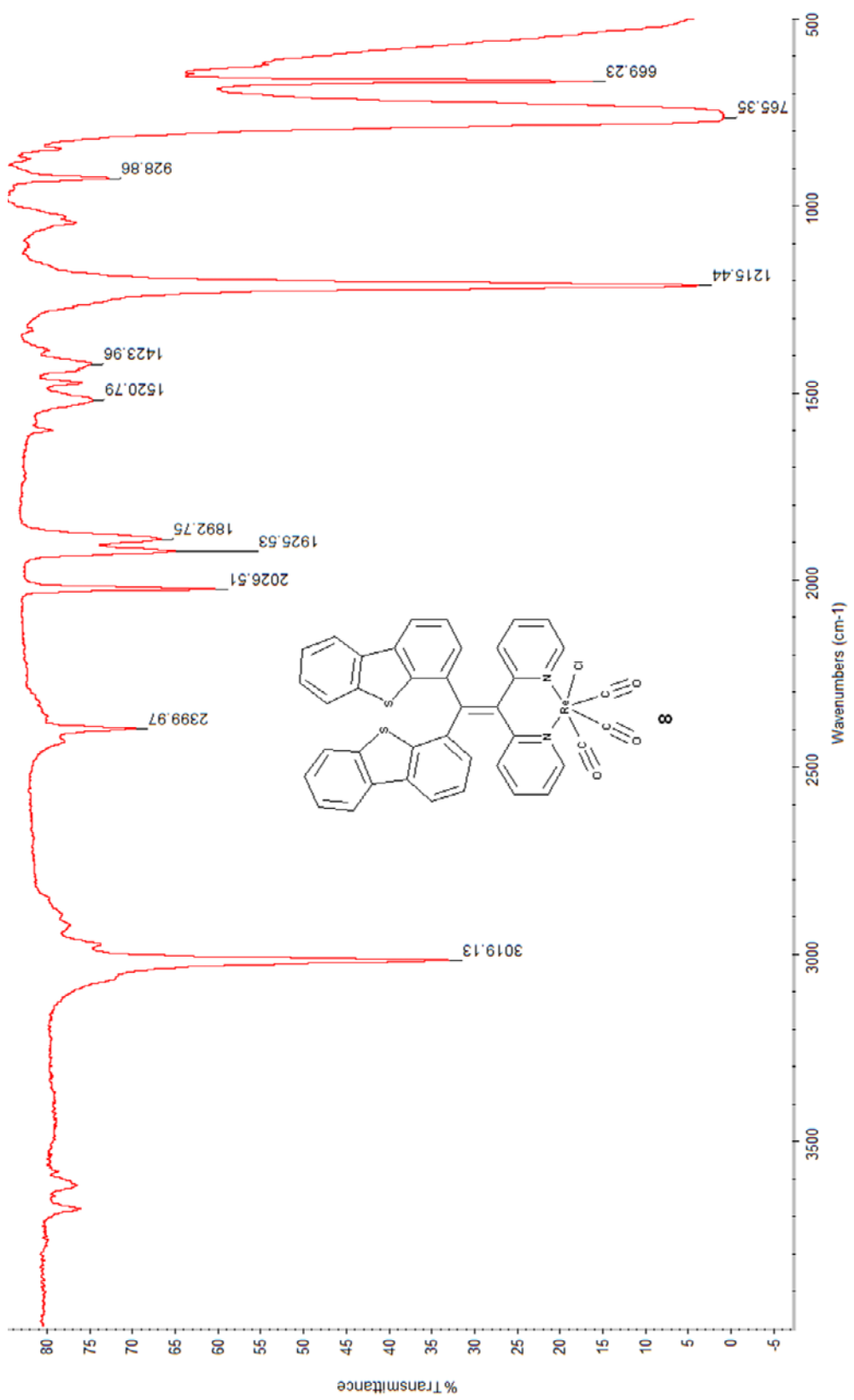


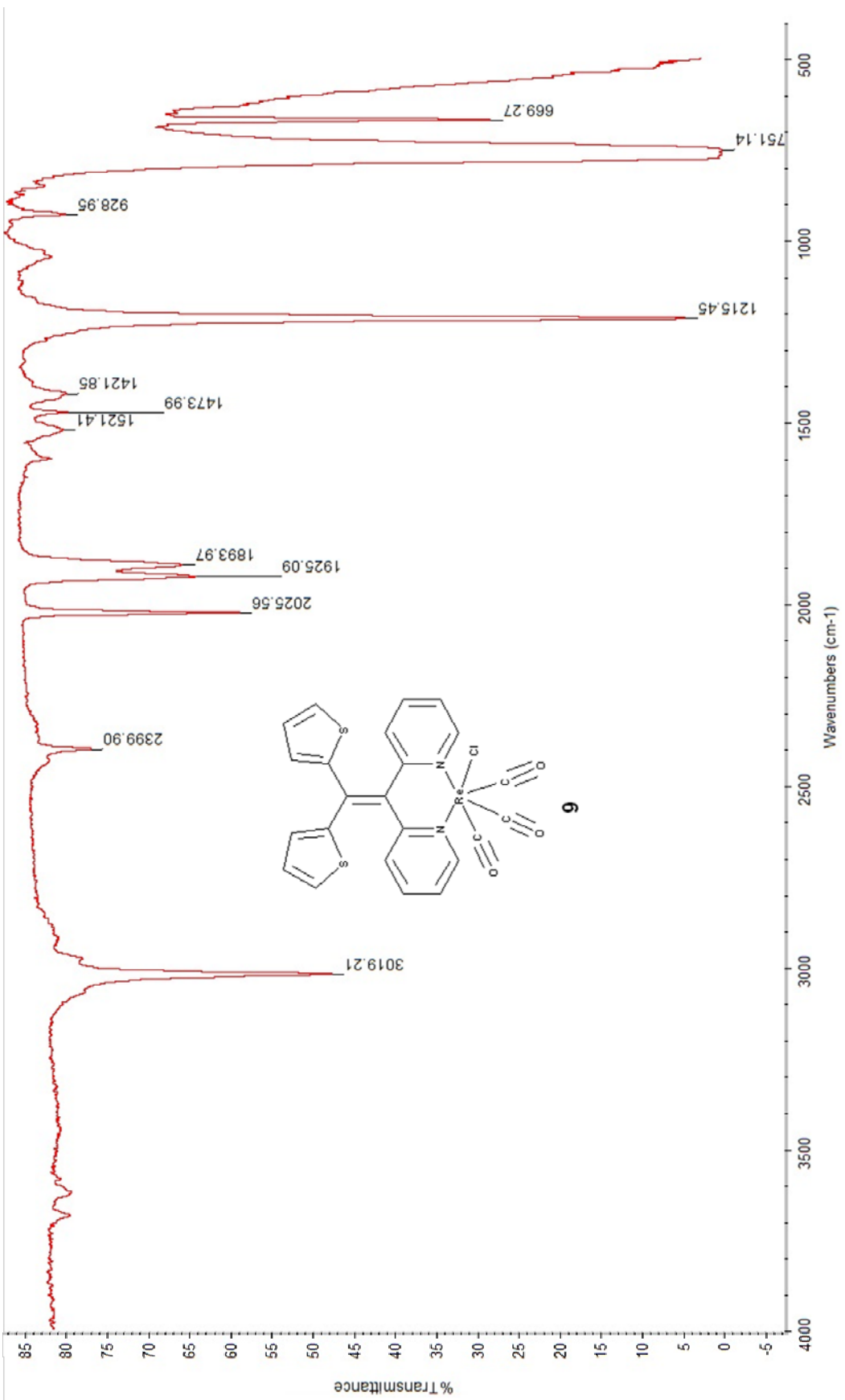
Figure S45. ORTEP plot of **12**·toluene.

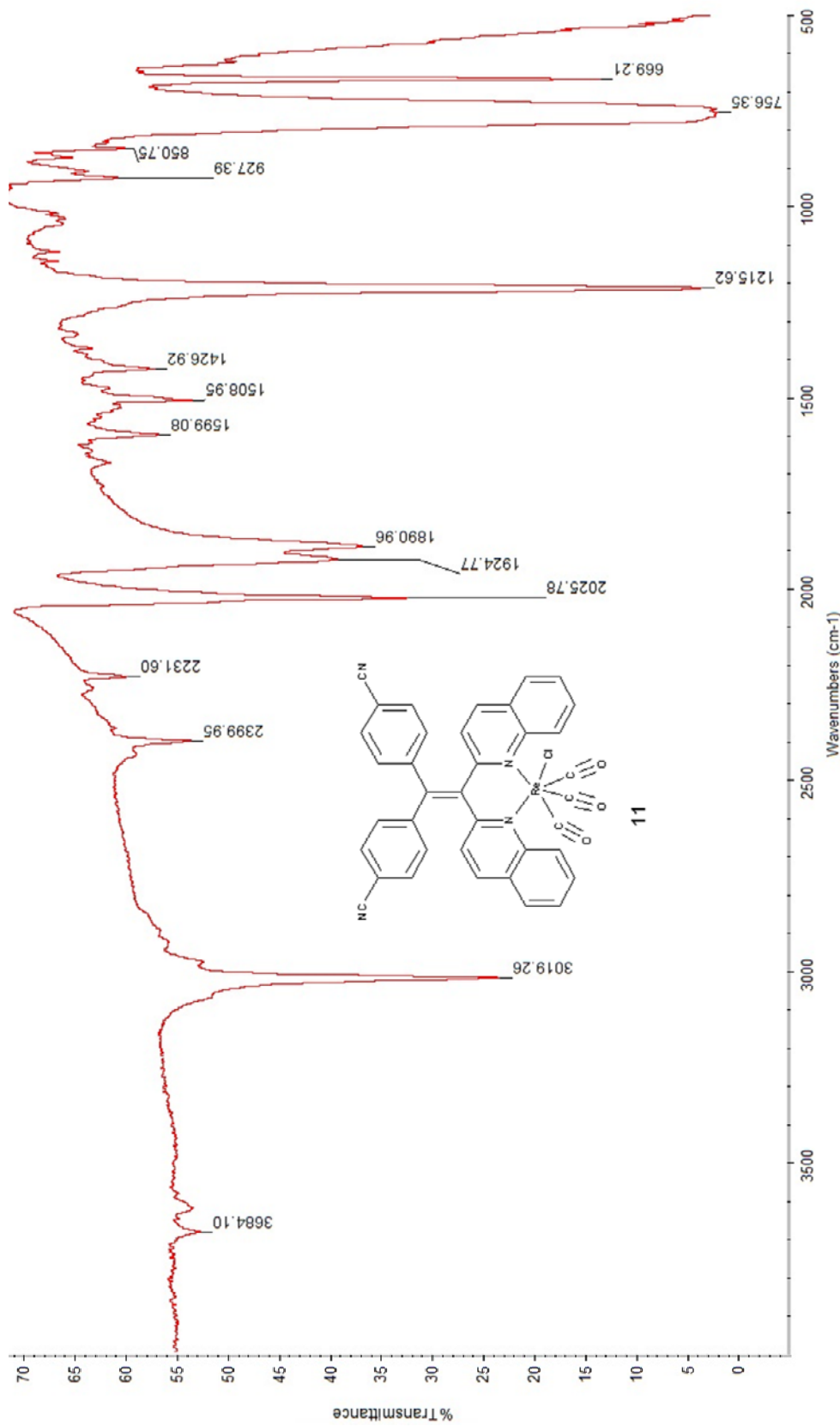
References:

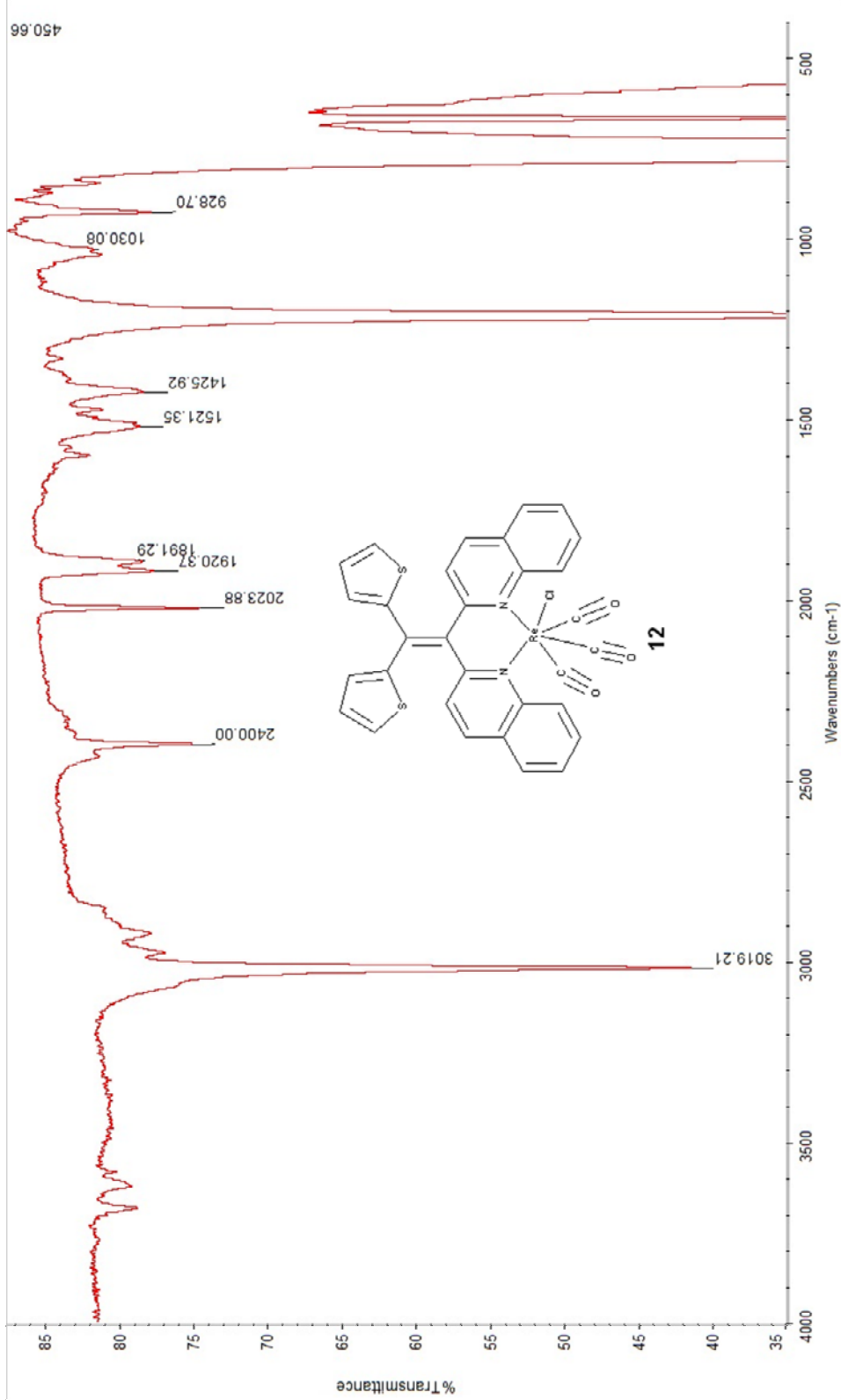
1. K. Nakamaru, *Bull. Chem. Soc. Jpn.*, 1982, **55**, 2697-2705.

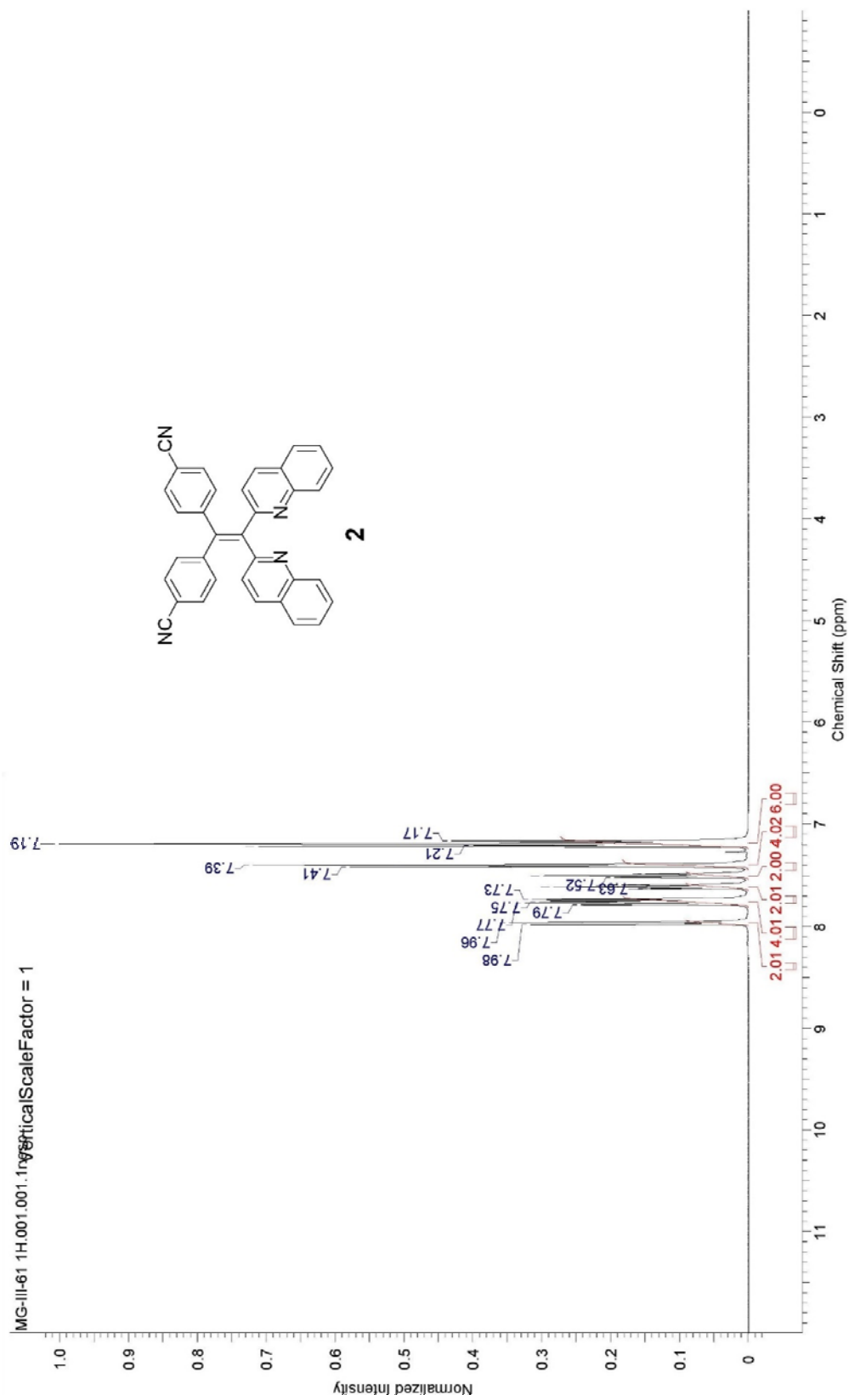


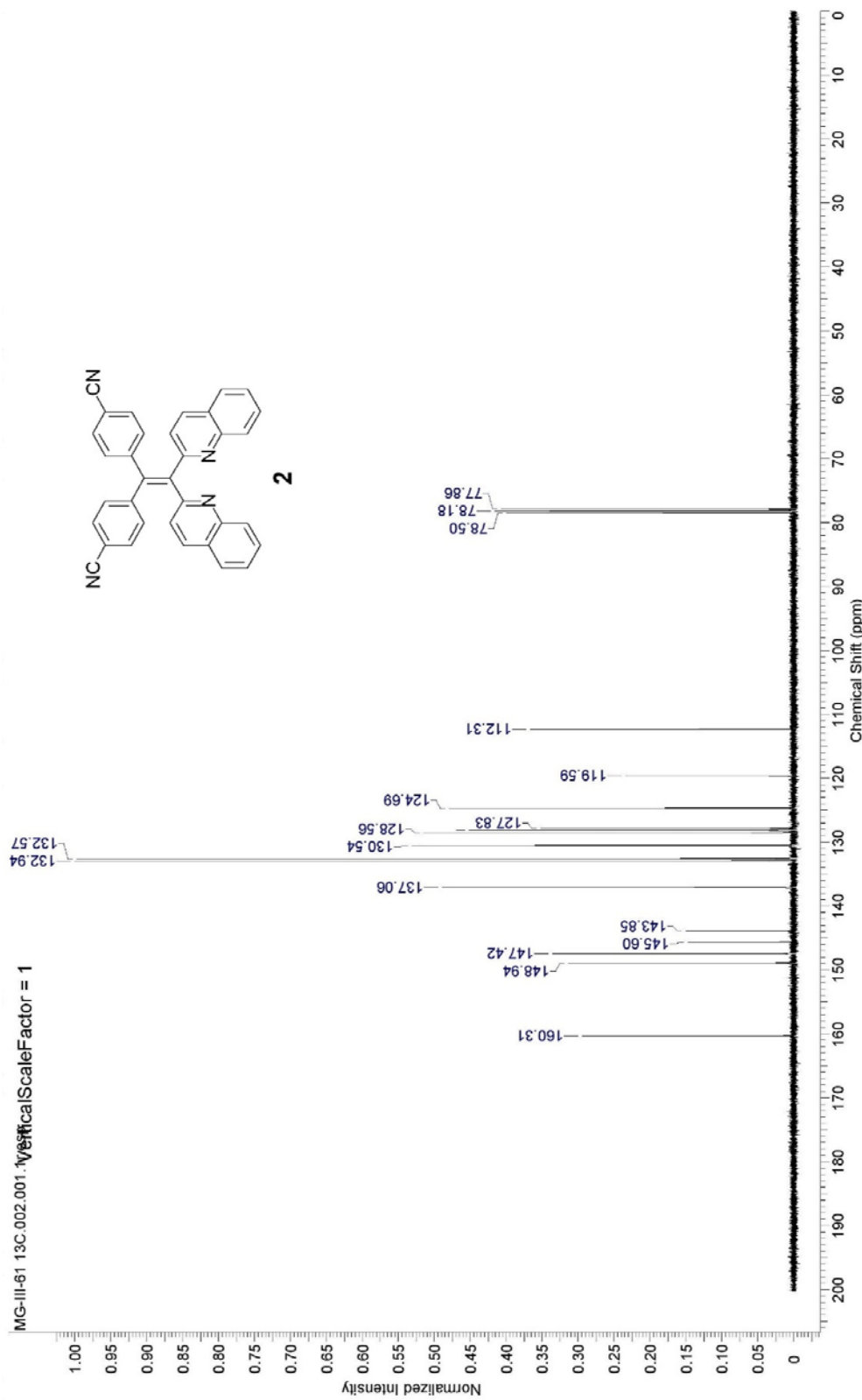


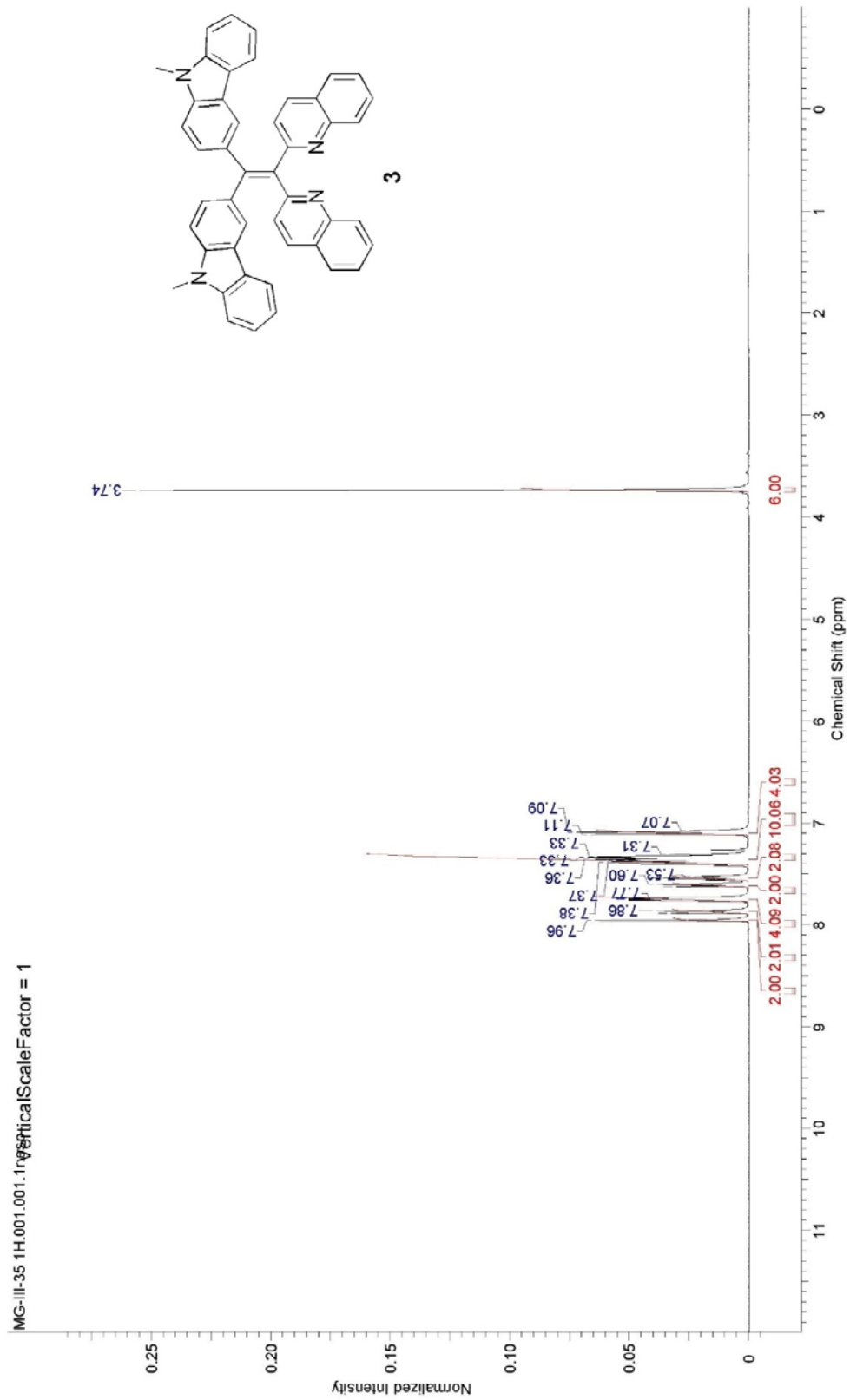
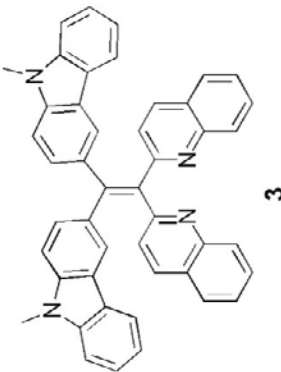


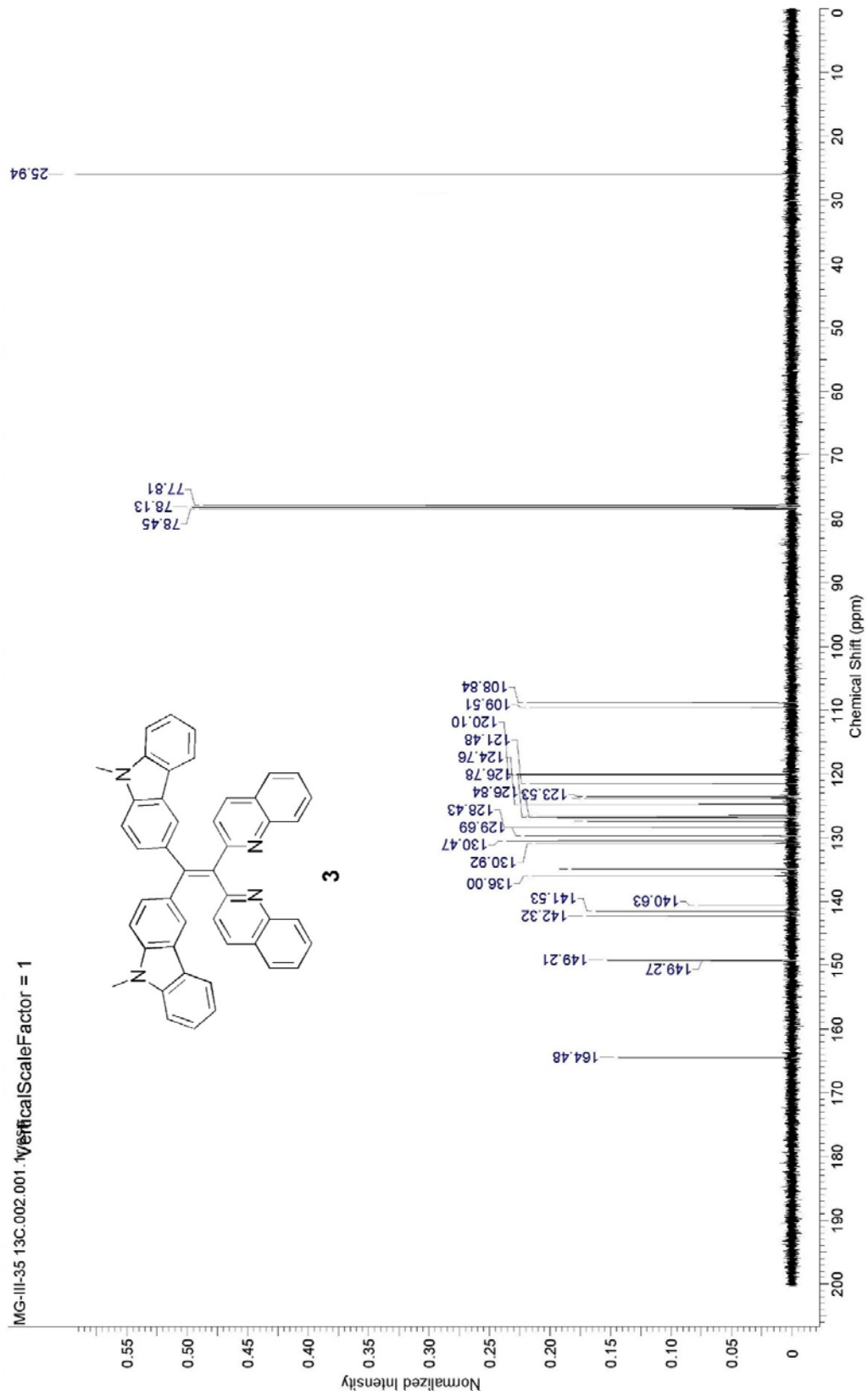


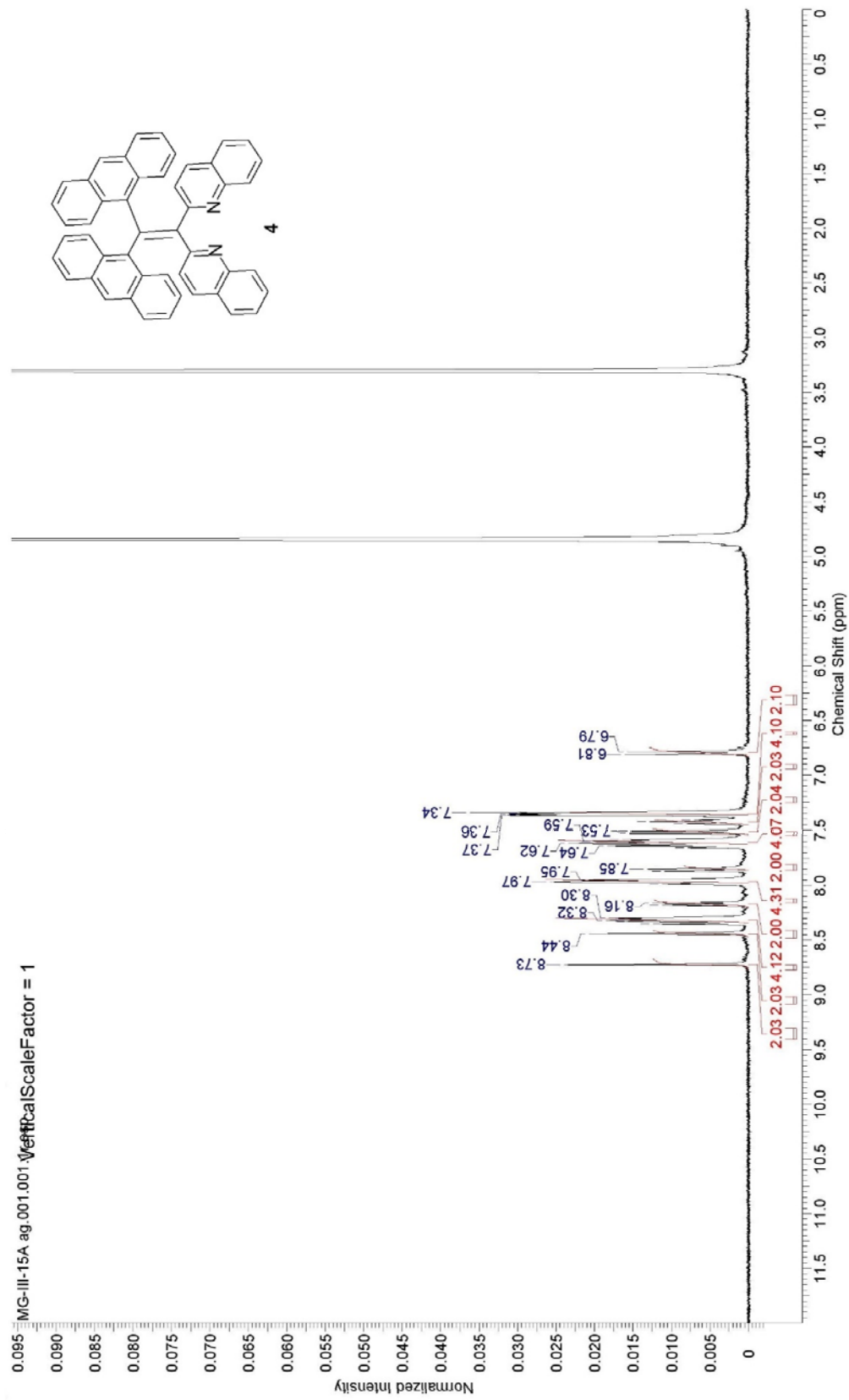
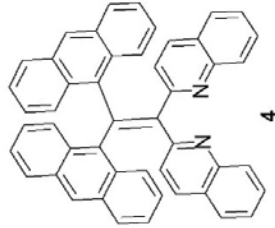


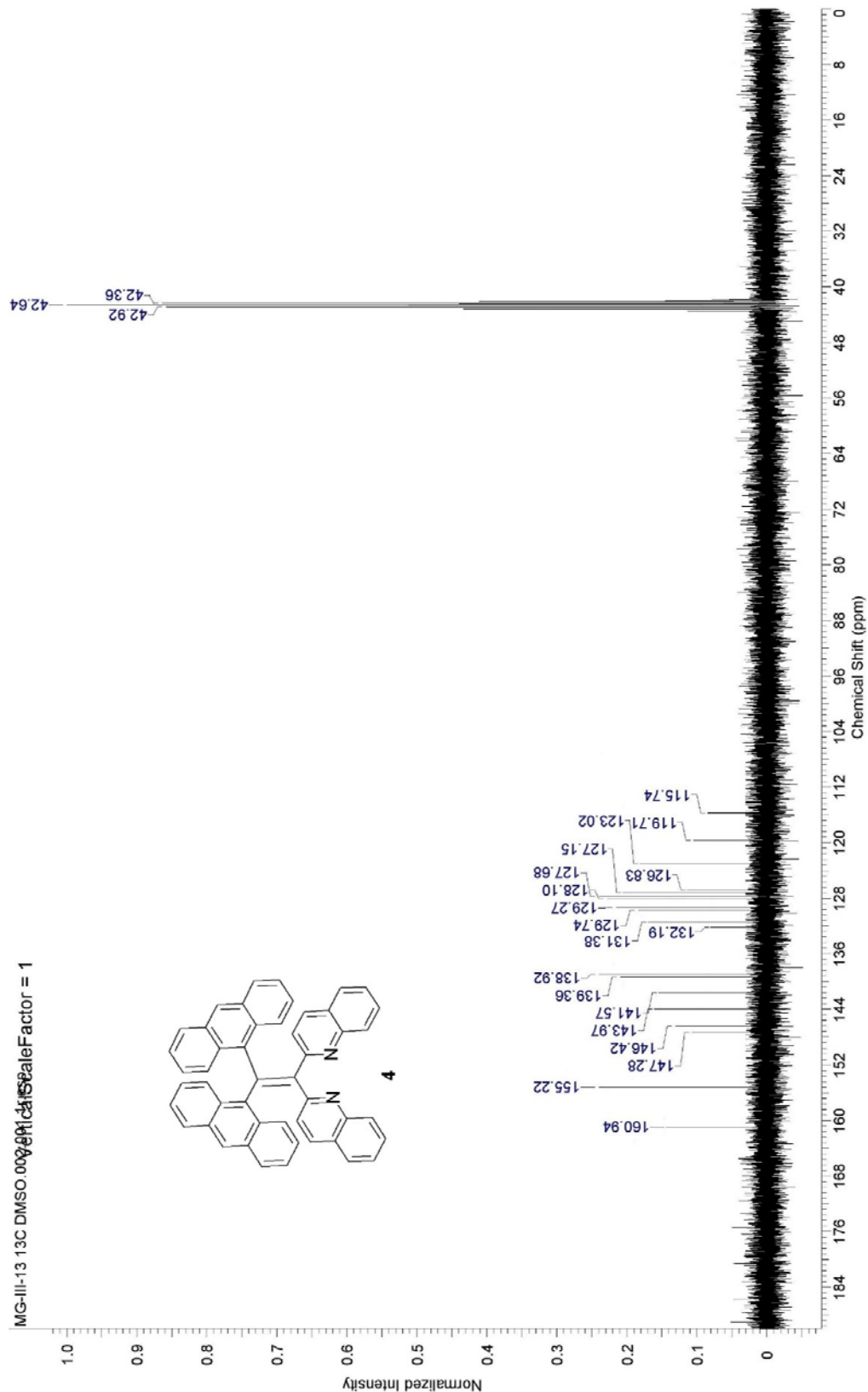


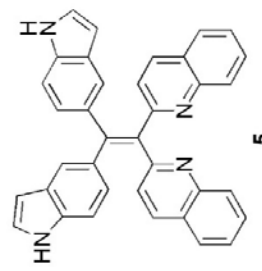




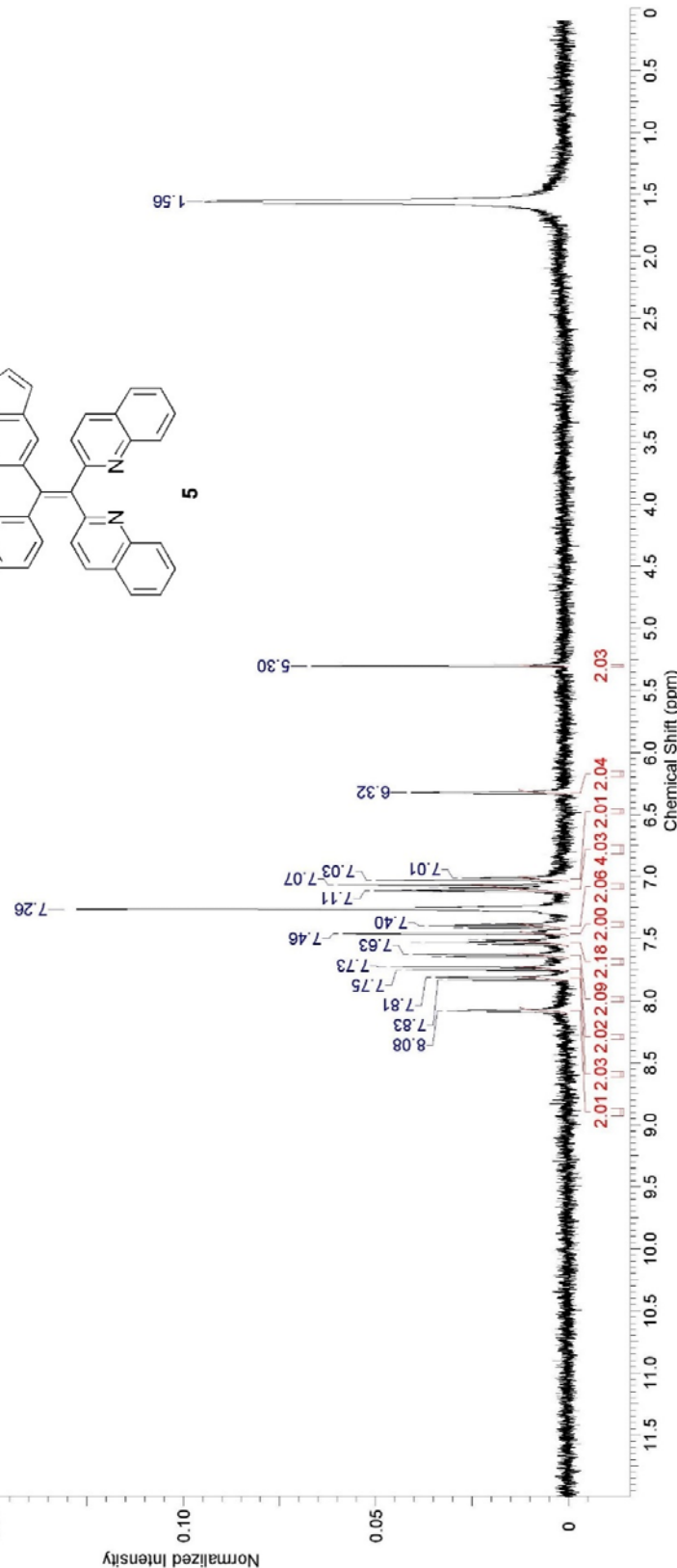


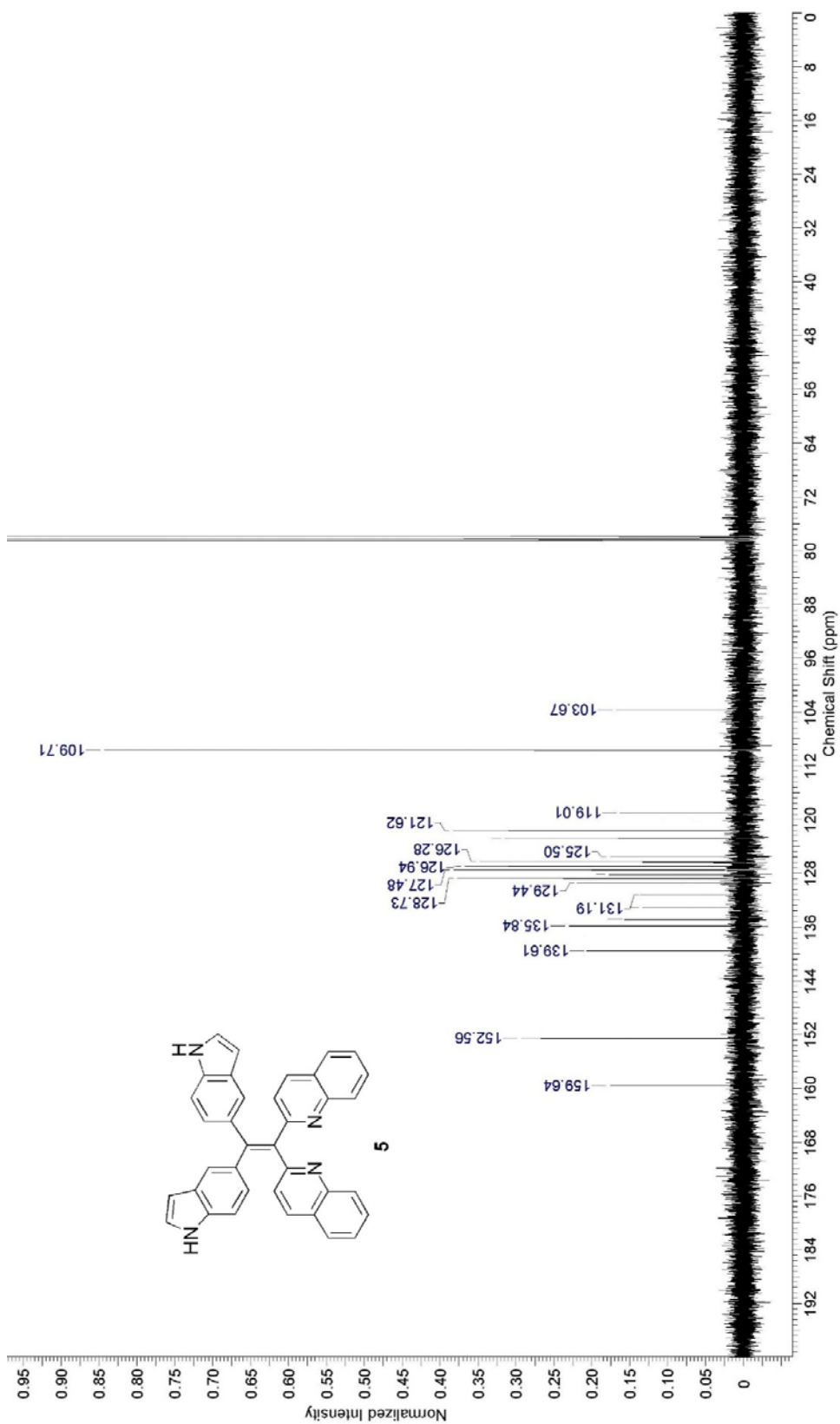


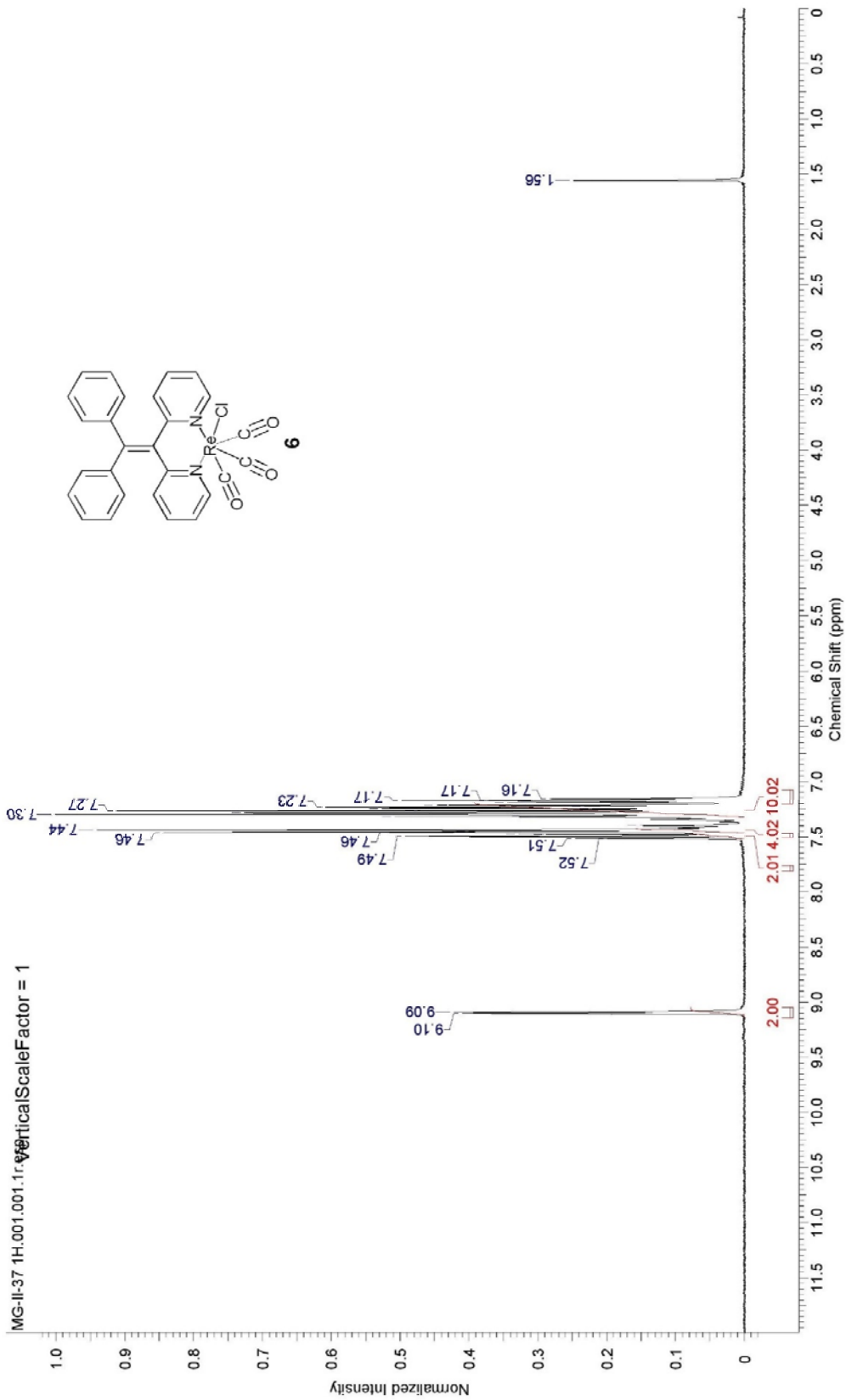


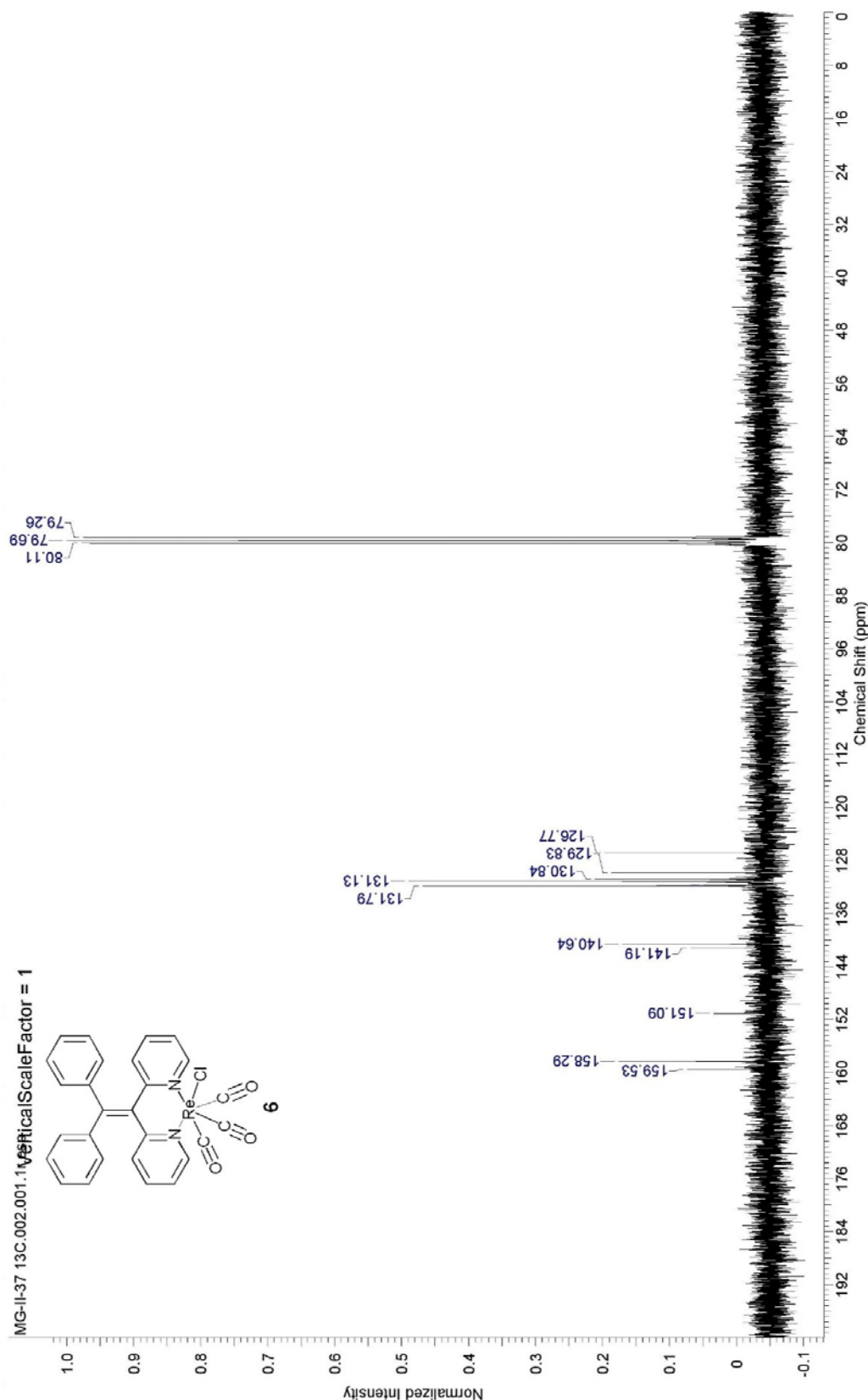
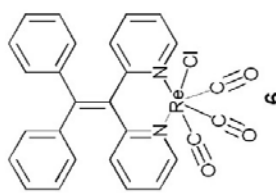


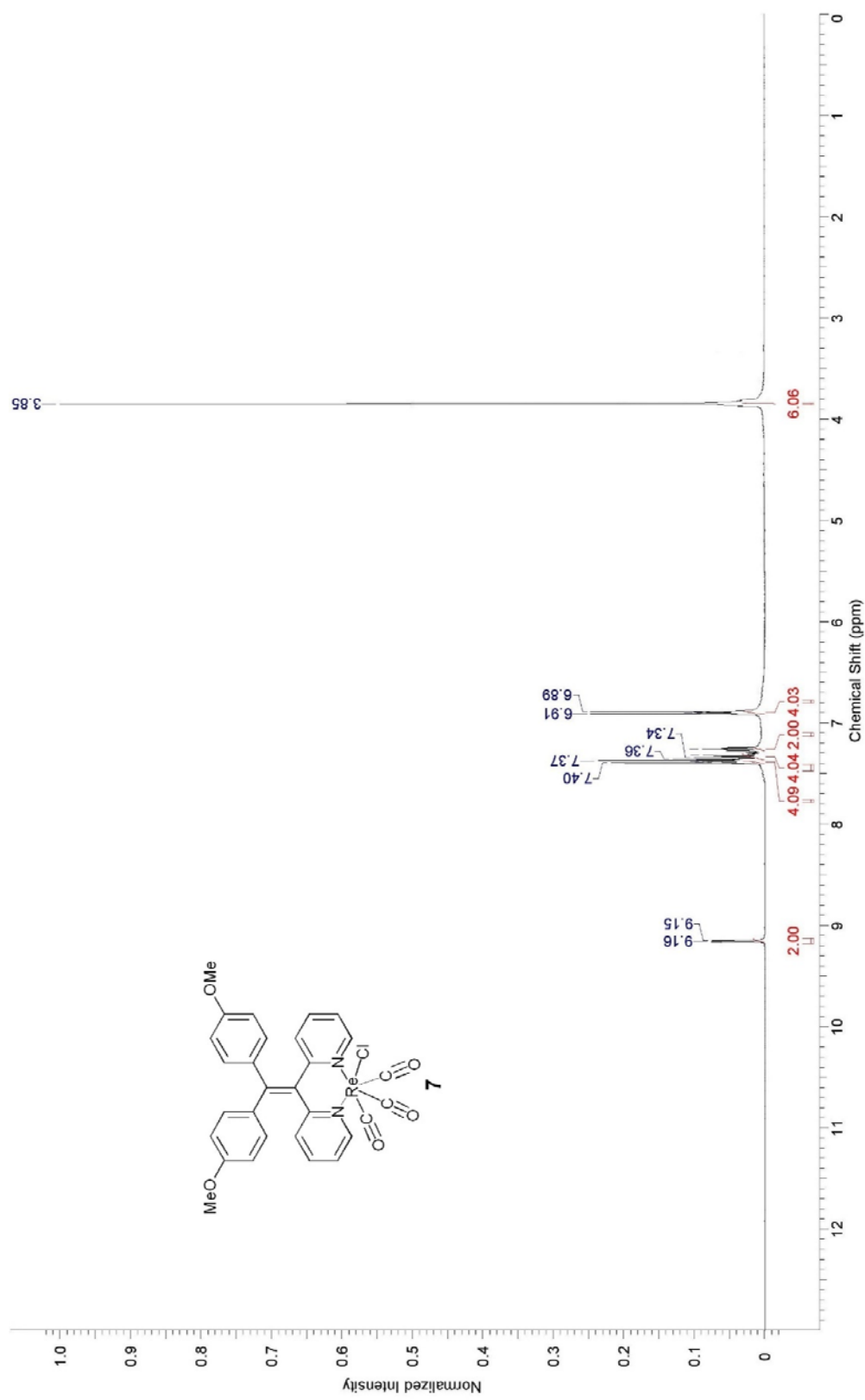
5

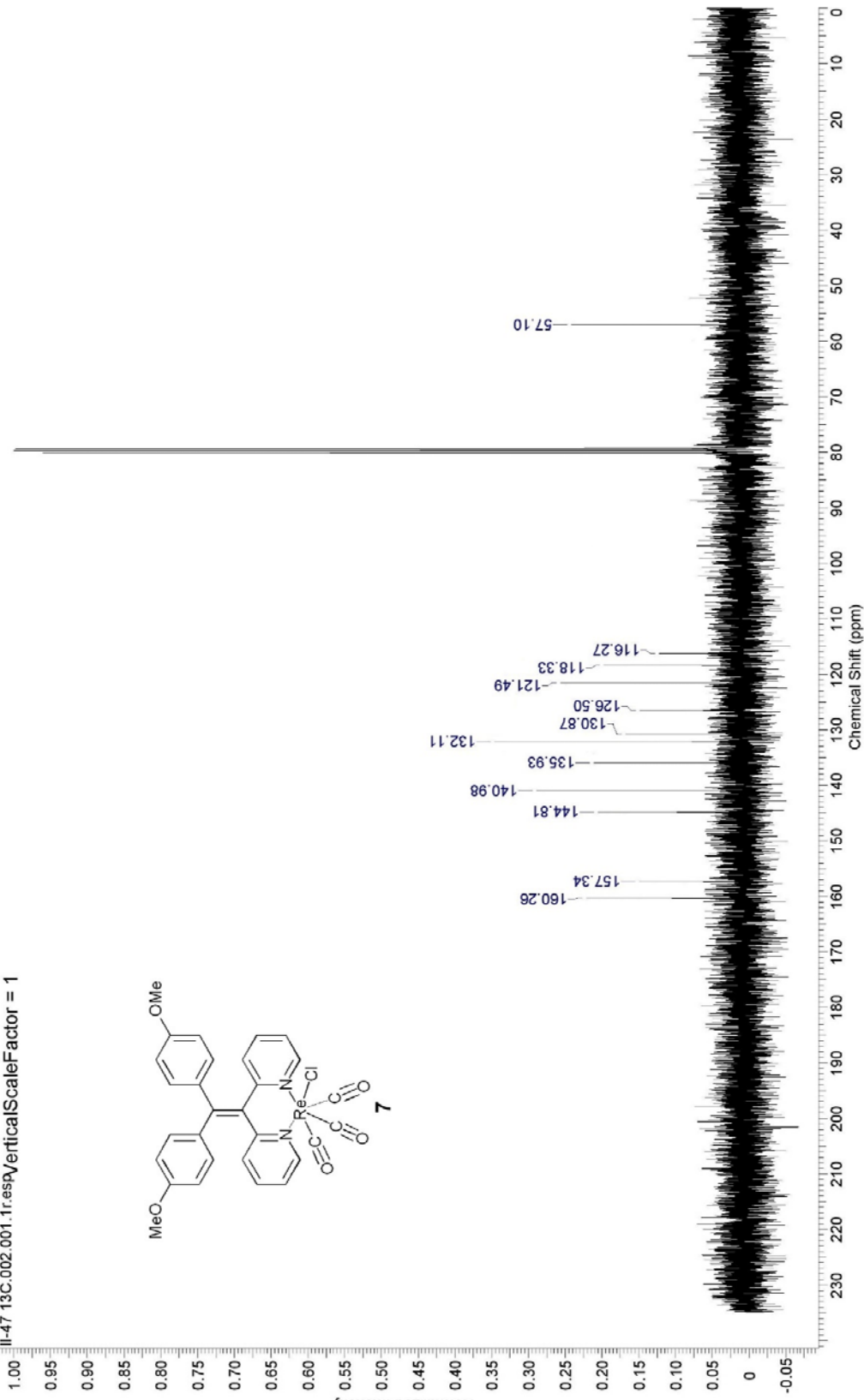




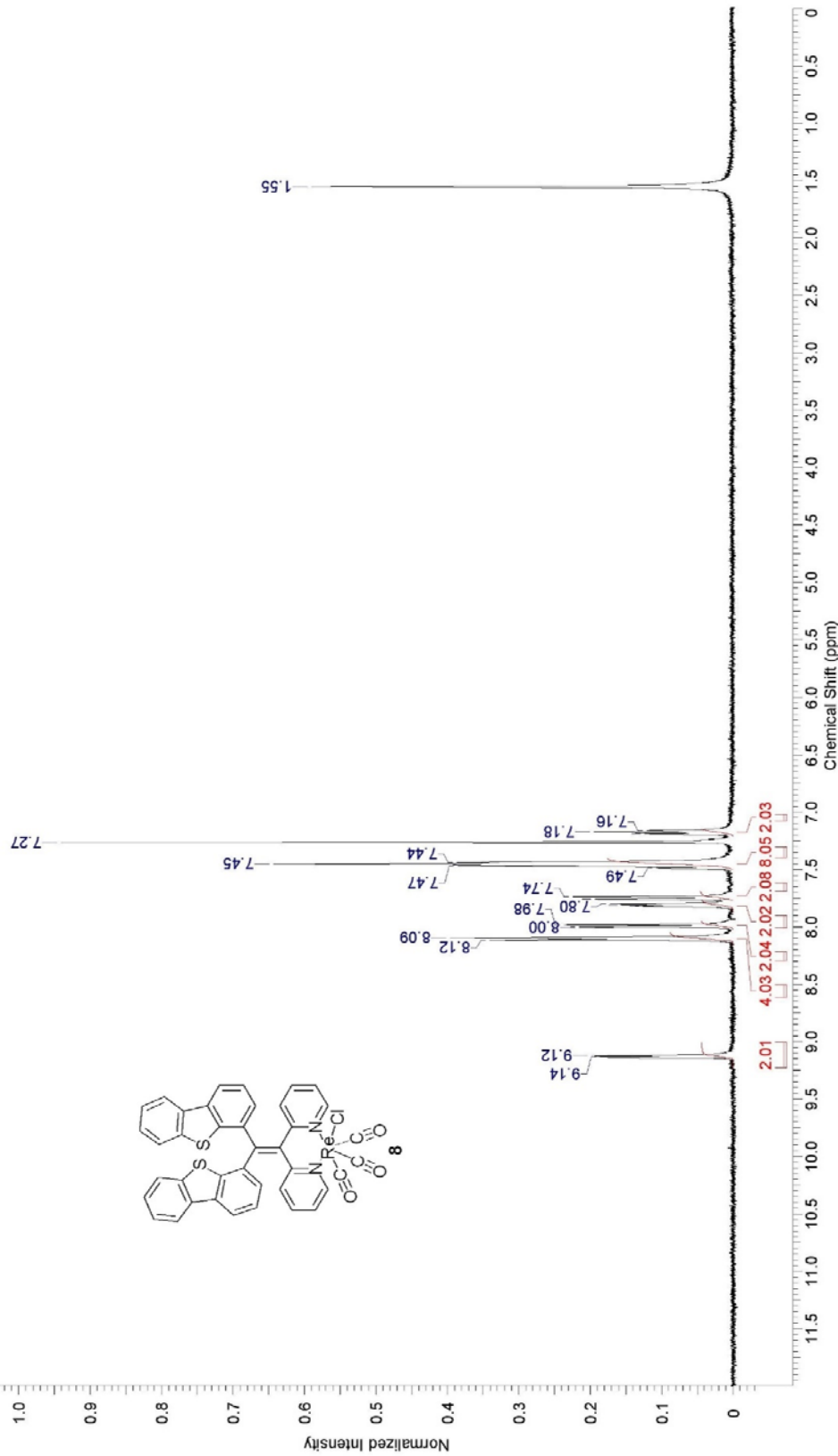


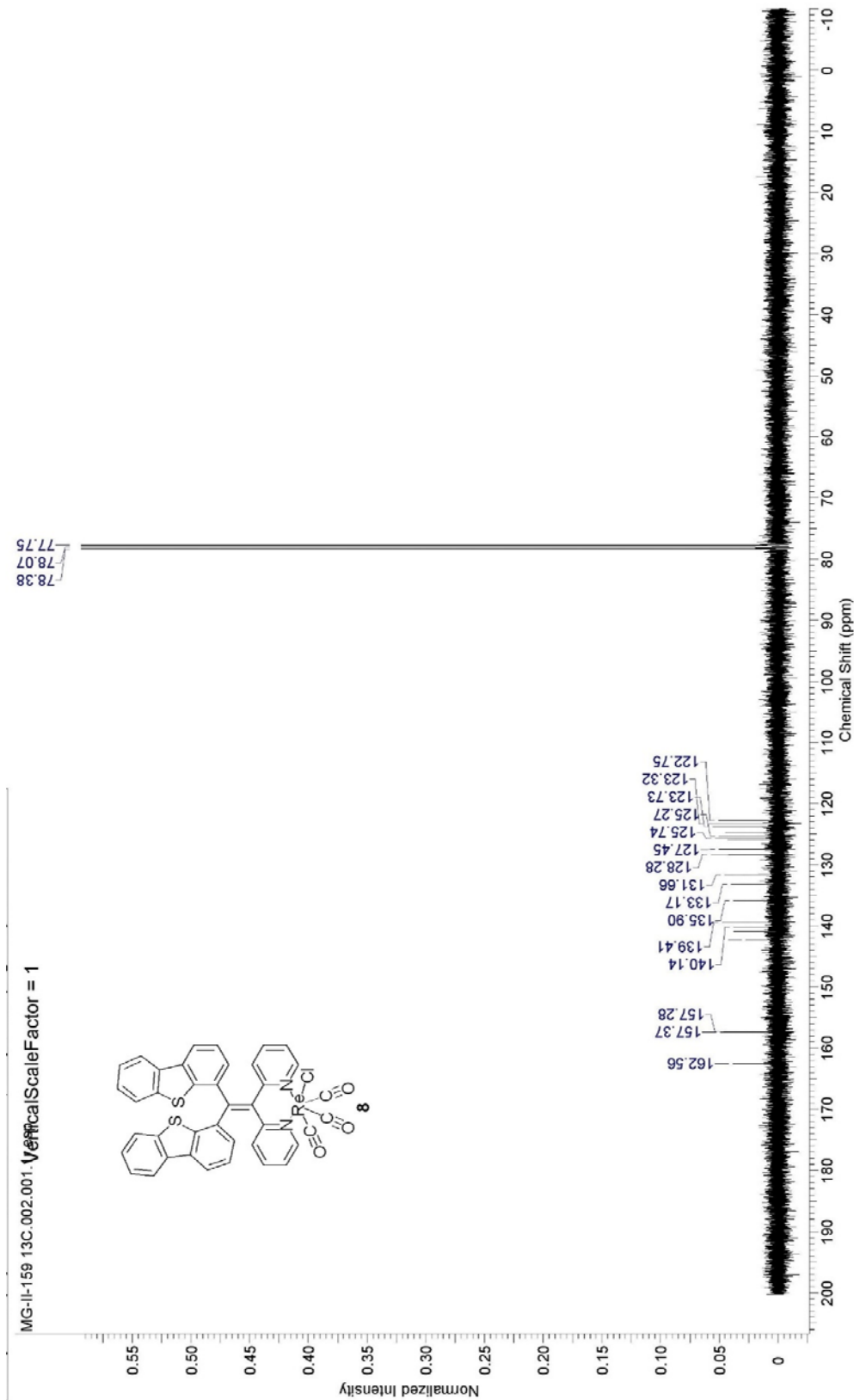




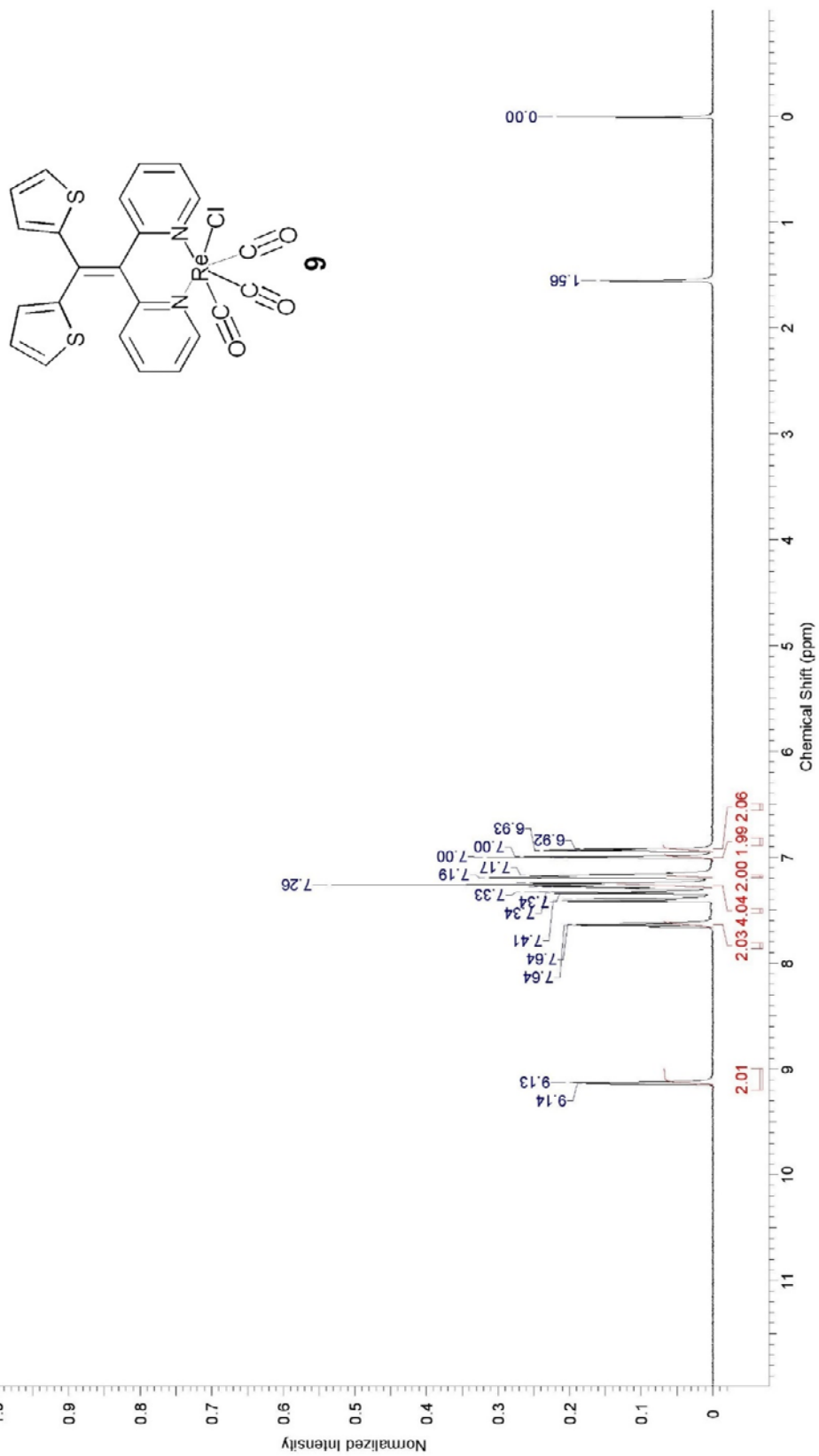


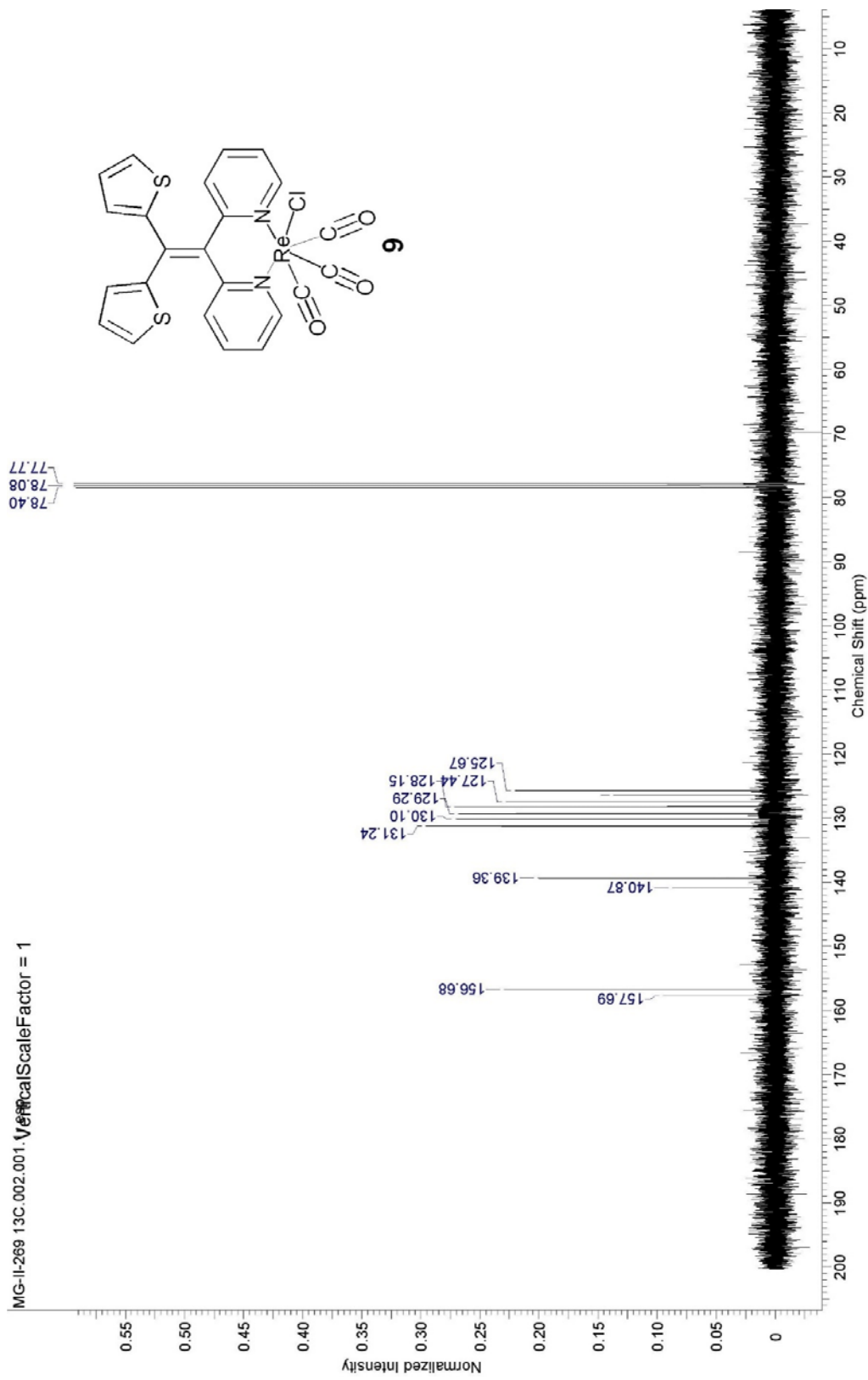
MG-II-159 1H.001.001.149 PracticalScaleFFactor = 1



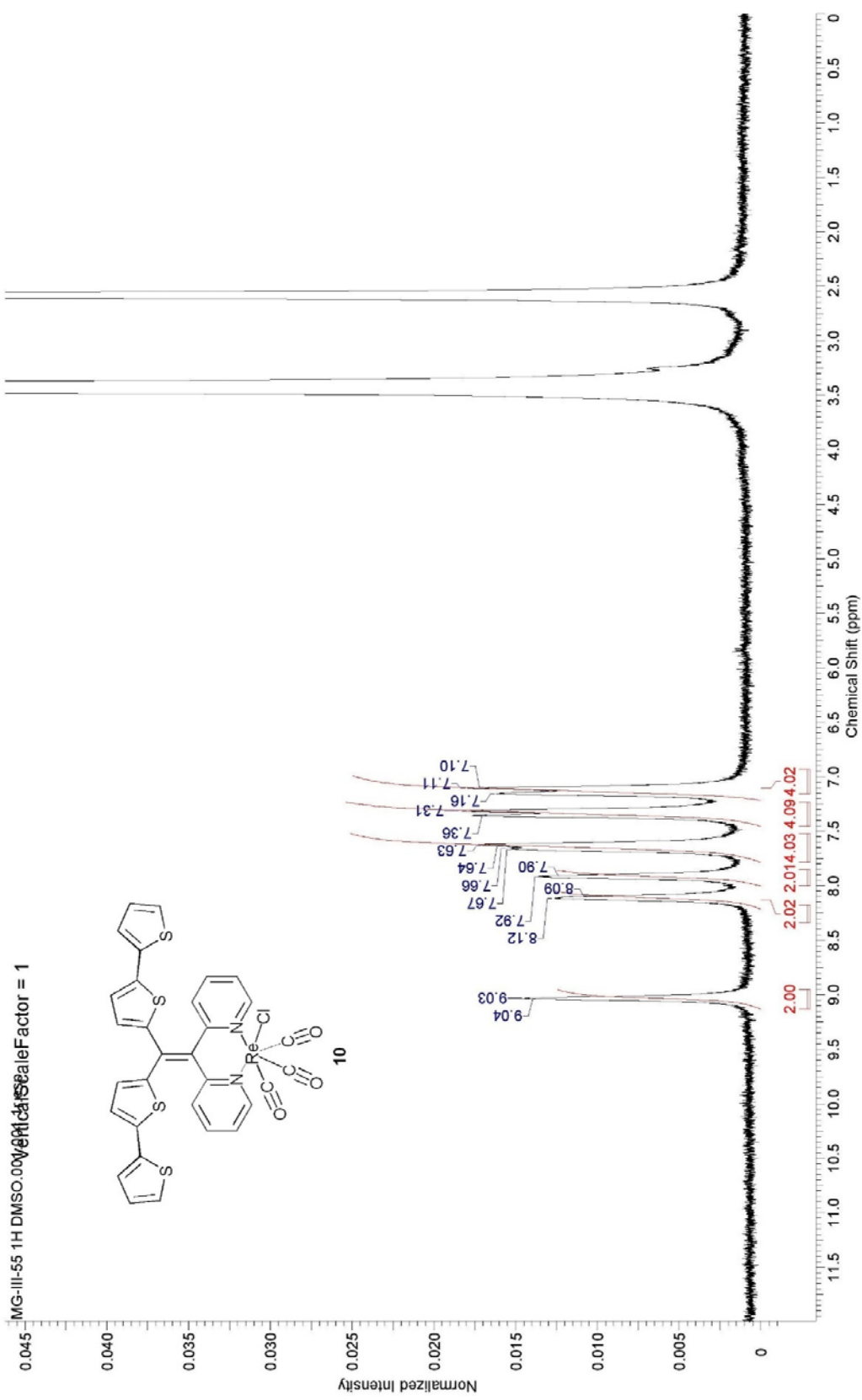


MG-II-289 1H.001.001.1\n&ScaleFactor = 1

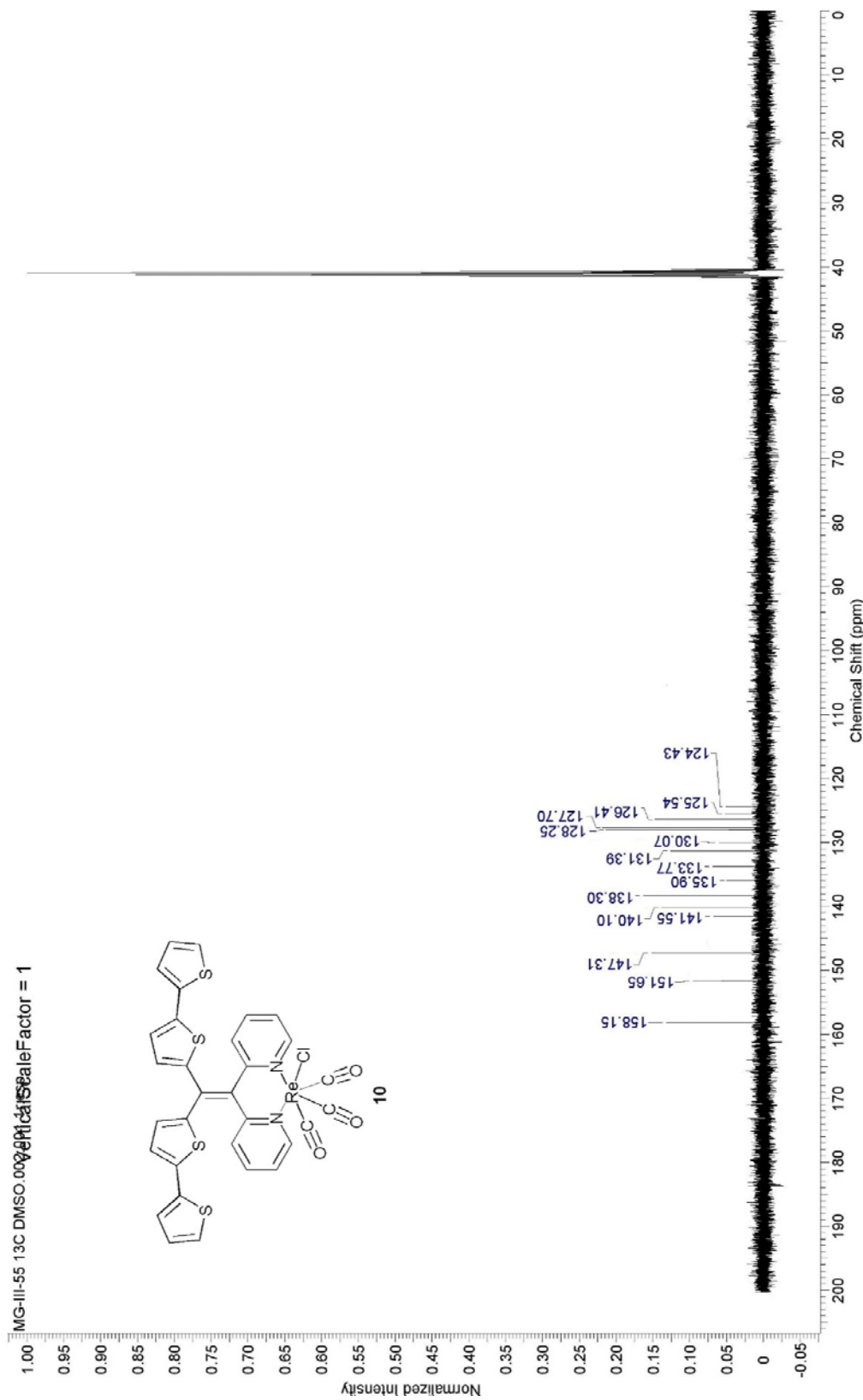




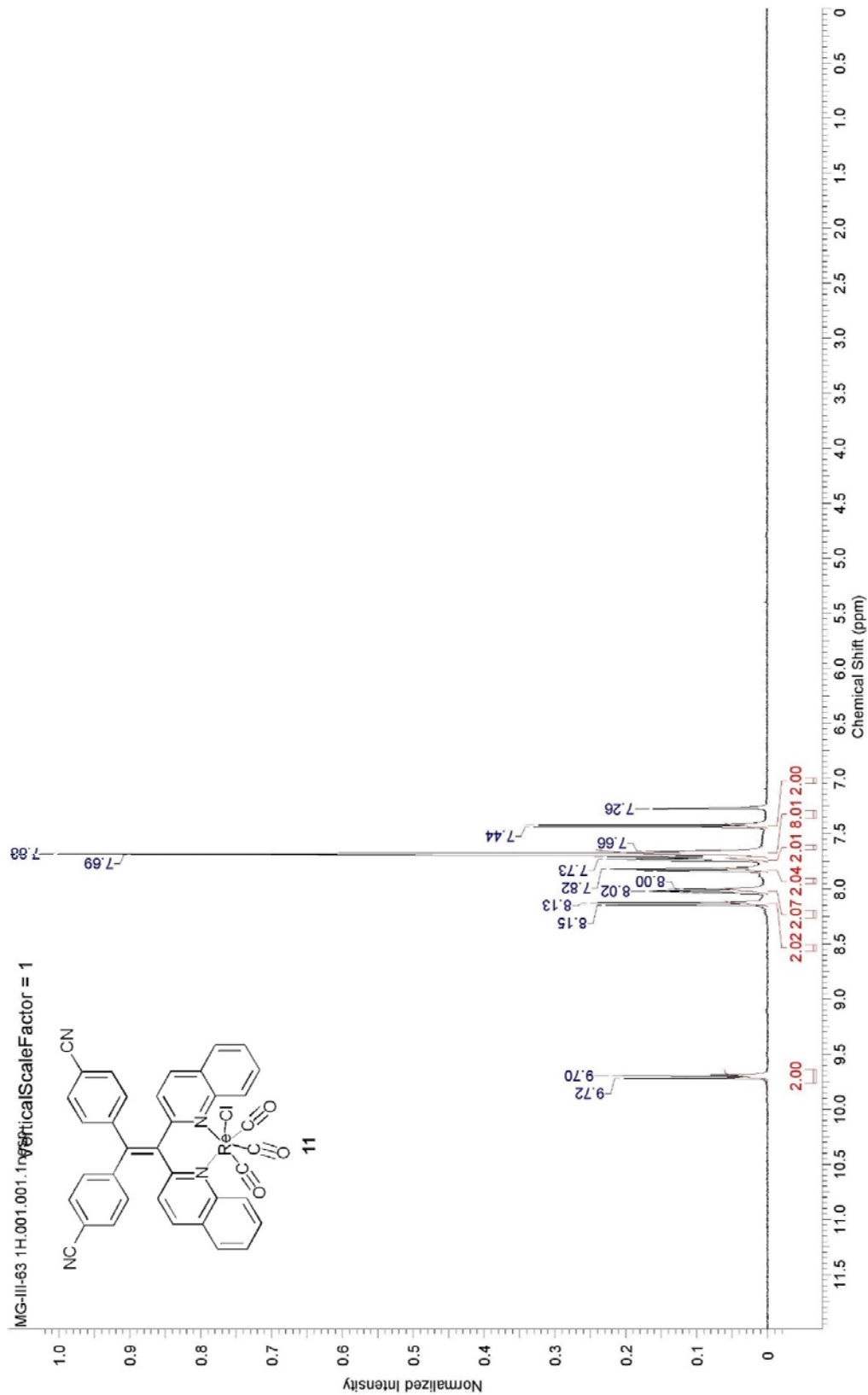
MG-III-55 1H DMSO.00W0R1c5ScaleFactor = 1

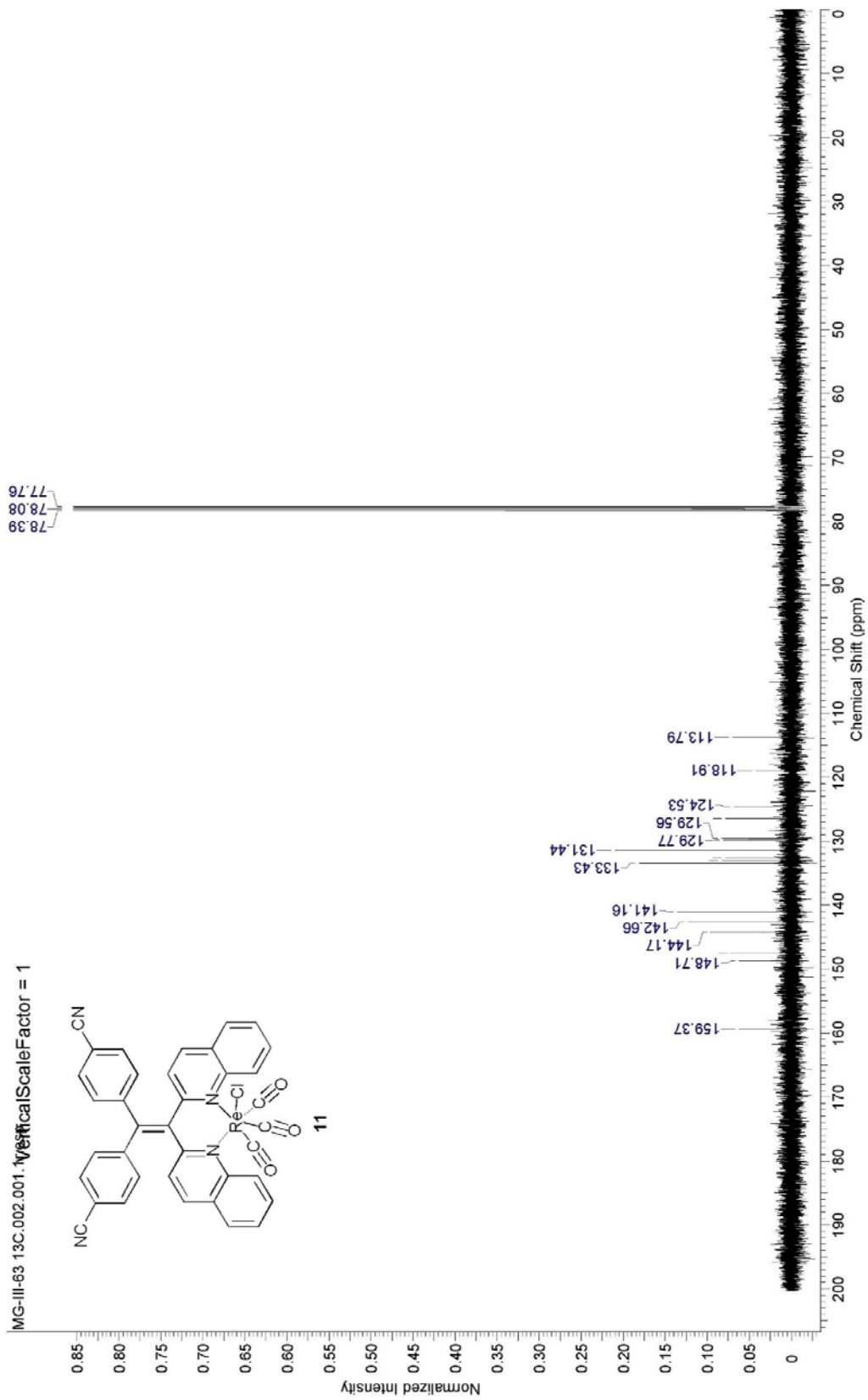


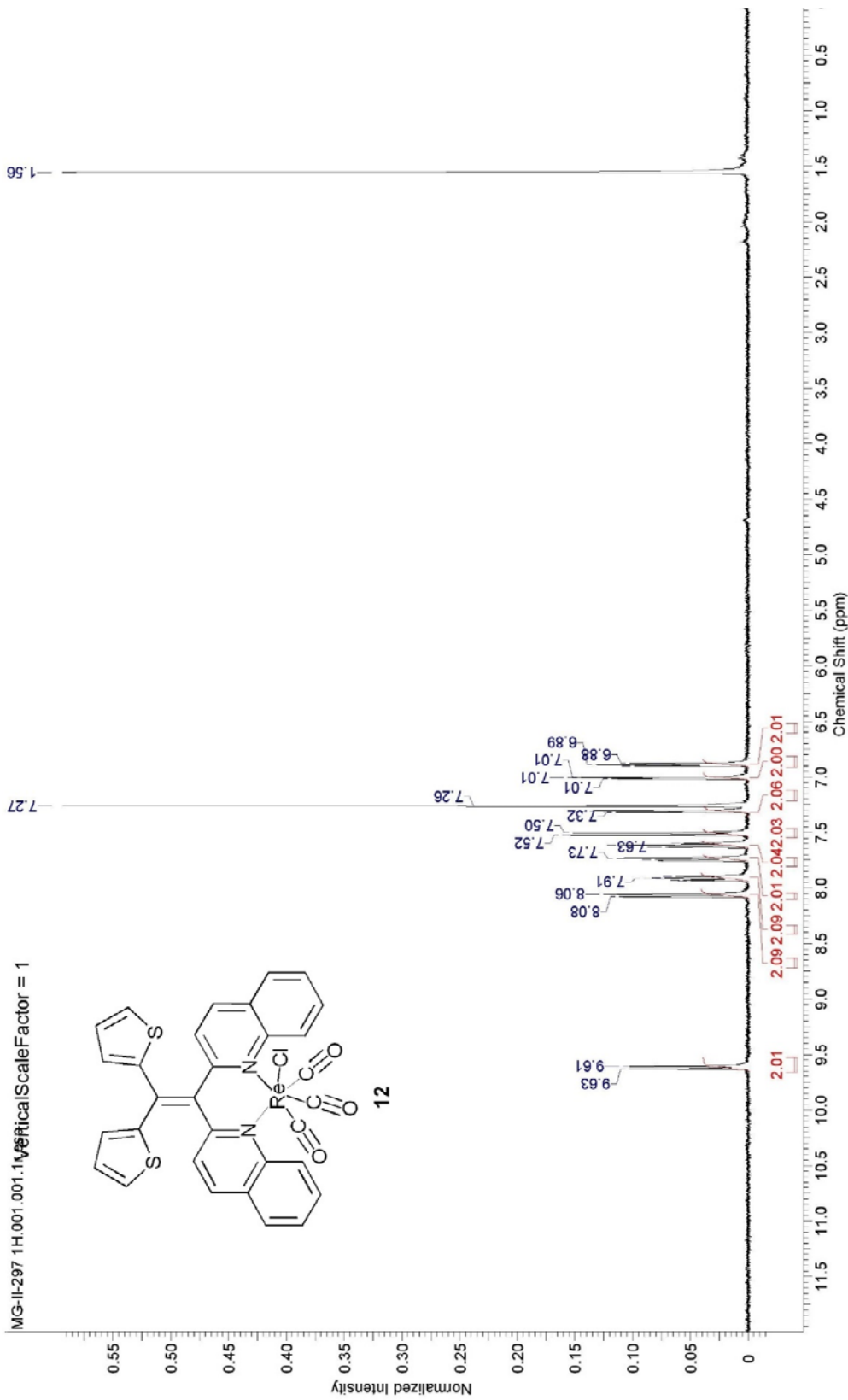
MG-III-55 13C DMSO.0078RI*ScaleFactor = 1

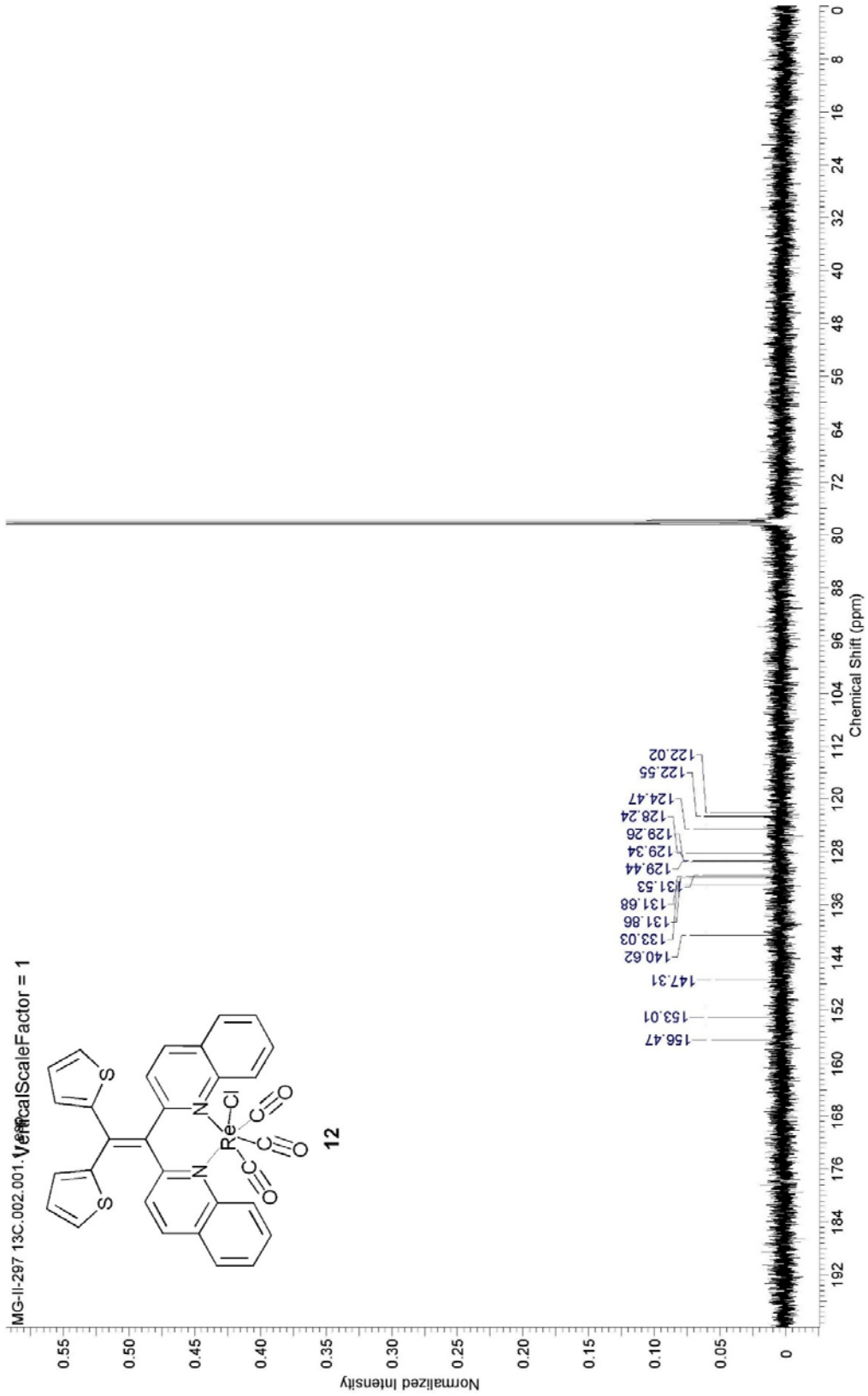


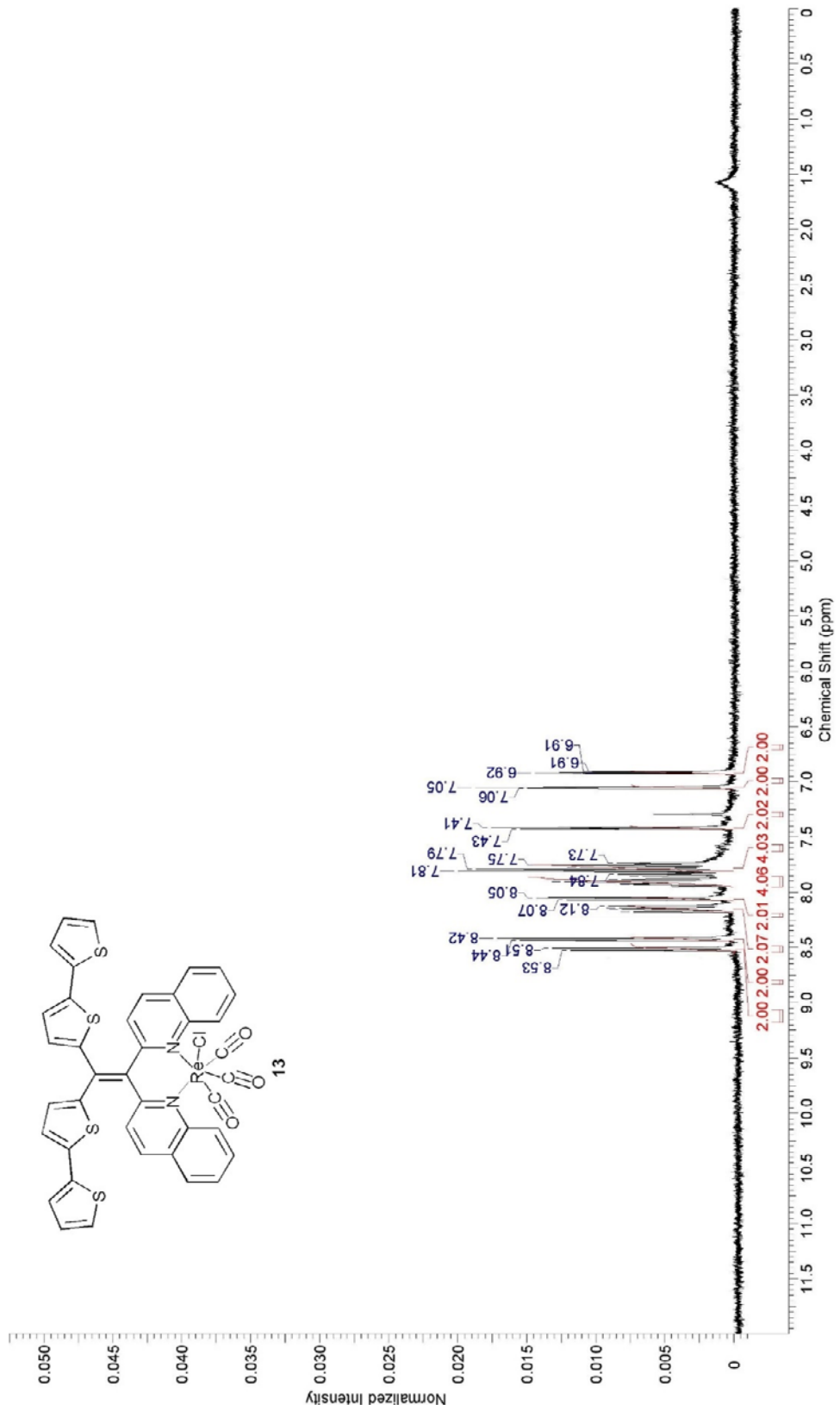
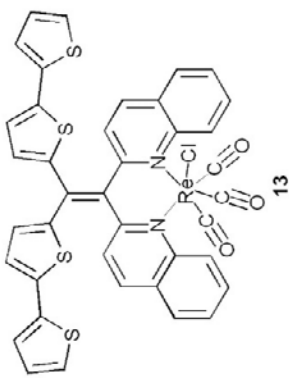
MG-III-63 1H,001.001.1ngSyntheticScaleFactor = 1

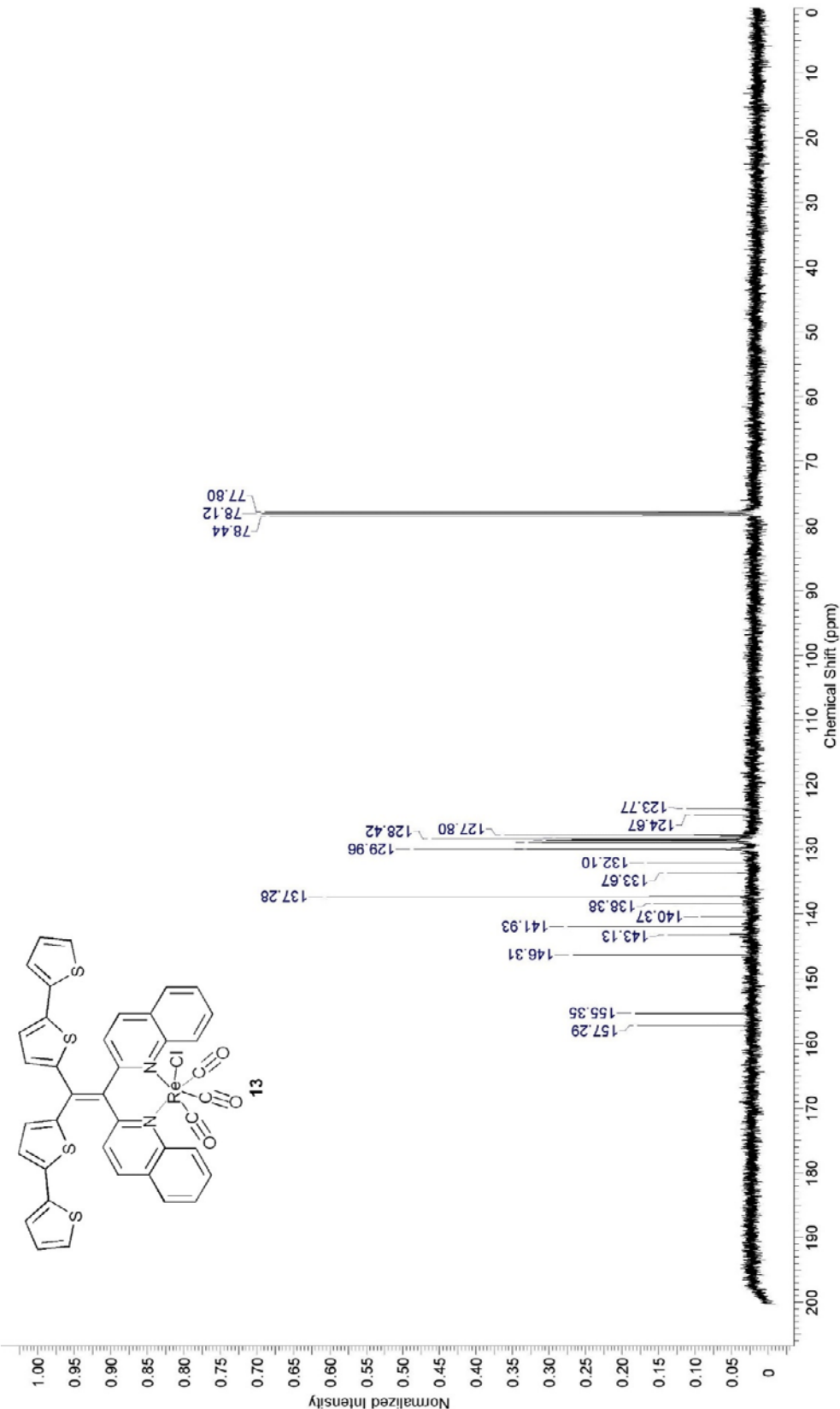


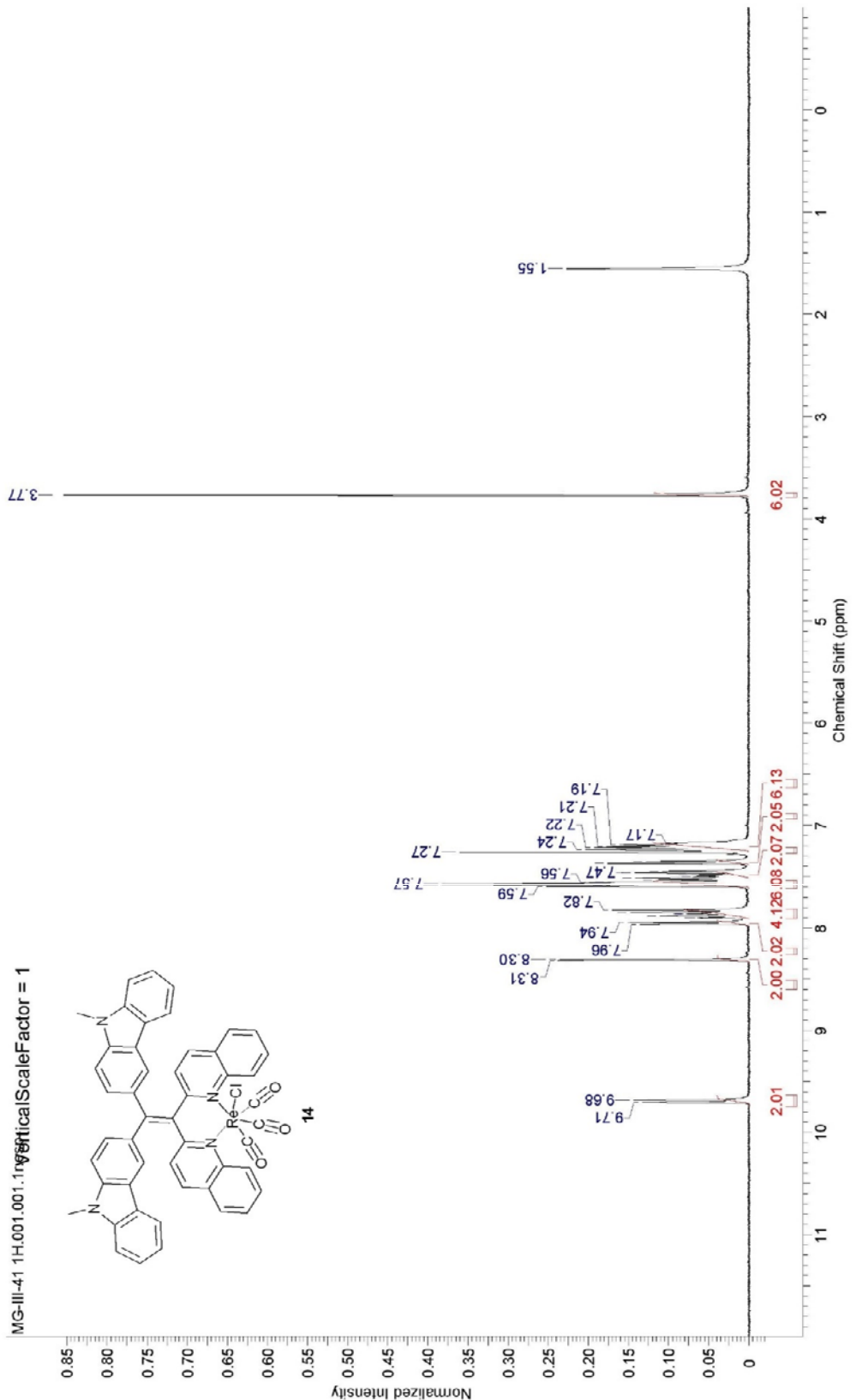


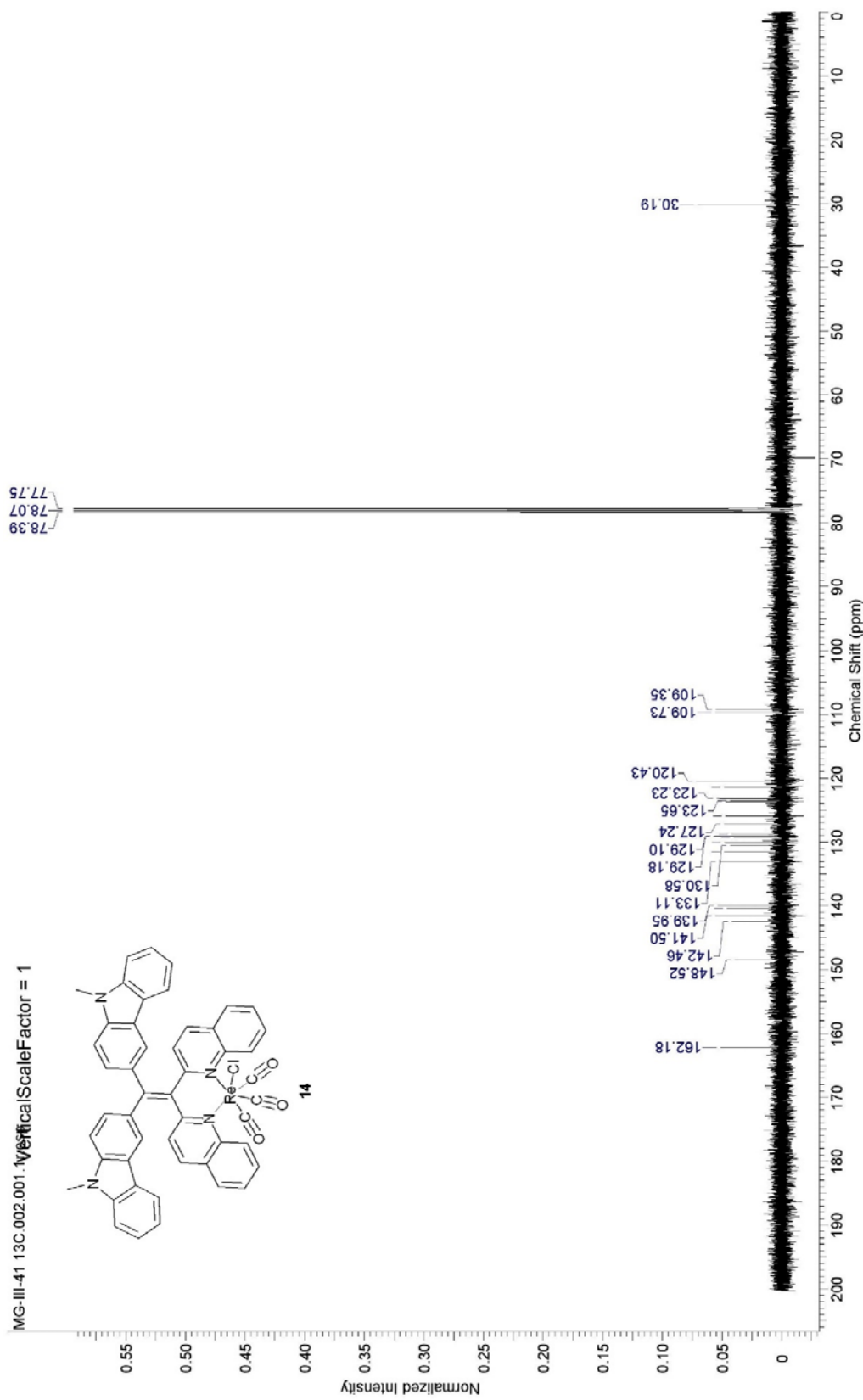












MG-III-19 H DMSO ag. 89% Purity Scale Factor = 1

